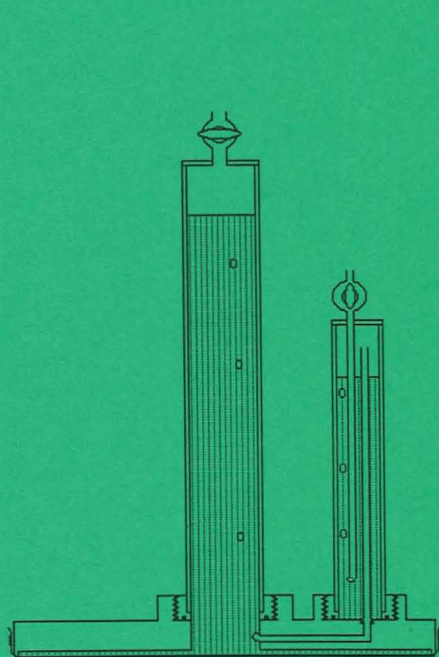




Influence of Slope Gradient and Aspect on Soil Hydraulic Conductivity Measured with Tension Infiltrometer

Field study in the Central Zone of Chile

Manuel Casanova P.



MSc Thesis (Examensarbete)

Supervisors (Handledare) : **Abraham Joel & Ingmar Messing**

Institutionen för markvetenskap
Avdelningen för lantbrukets hydroteknik

Swedish University of Agricultural Sciences
Department of Soil Sciences
Division of Agricultural Hydrotechnics

Avdelningsmeddelande 98:3
Communications

Uppsala 1998

ISSN 0282-6569

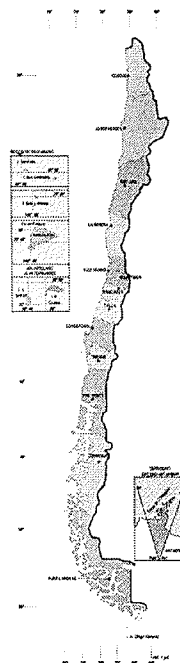
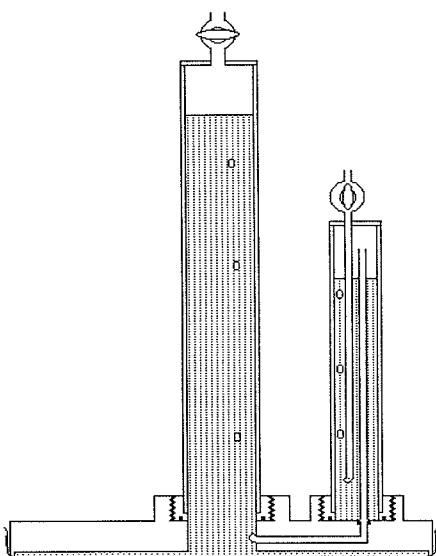
ISRN SLU-HY-AVDM--98/3--SE



Influence of Slope Gradient and Aspect on Soil Hydraulic Conductivity Measured with Tension Infiltrometer

Field study in the Central Zone of Chile

Manuel Casanova P.



MSc Thesis (Examensarbete)

Supervisors (Handledare) : **Abraham Joel & Ingmar Messing**

**Institutionen för markvetenskap
Avdeleningen för lantbrukets hydroteknik**

**Swedish University of Agricultural Sciences
Department of Soil Sciences
Division of Agricultural Hydrotechnics**

**Avdelningsmeddelande 98:3
Communications**

Uppsala 1998

ISSN 0282-6569

ISRN SLU-HY-AVDM--98/3--SE

CONTENTS

Abstract	7
Resumen	7
Acknowledgment	8
1. INTRODUCTION	9
2. SCOPE OF WORK	9
2.1 Objective	9
3. THEORY	10
3.1 Infiltration theory	10
3.2 Factors affecting infiltration rate	11
3.3 Characteristics of tension infiltrometer	12
3.4 Tension infiltrometer theory	13
4. MATERIALS AND METHODS	17
4.1 Field work (Chile)	17
4.1.1 Physiography	17
4.1.2 Location	17
4.1.3 Geology and geomorphology	19
4.1.4 Climate	19
4.1.5 Vegetation	20
4.1.6 Study sites and treatments	20
4.2 Laboratory work (Ultuna - Sweden).	22
4.2.1 Soil	22
4.2.2 Treatments	22
4.3 Treatment of the data	23
5. RESULTS AND DISCUSSION	24
5.1 Field work results	24
5.2 Laboratory results	30
5.3 Discussion	32
6. CONCLUSIONS	38
7. REFERENCES	39
APPENDIX 1 : <i>Climate</i>	43
APPENDIX 2 : <i>Topographic Survey</i>	46
APPENDIX 3 : <i>Soil description</i>	47
APPENDIX 4 : <i>Slope adjustment of tension infiltrometer</i>	50

Abstract

Casanova, M. 1998. Influence of slope gradient and aspect on soil hydraulic conductivity measured with tension infiltrometer. Field study in the Central Zone of Chile.

The tension infiltrometer is a device for measuring unsaturated hydraulic conductivity [$K(\psi)$] in the larger soil pores. By regulating the supply pressure head during infiltration with the help of a bubble tower, it is possible to control the size range of soil pores that transmit water. This technique was used in the characterization of infiltration in two rainfed hillsides (north and south exposure) of the central zone of Chile. The results showed smaller $K(\psi)$ values for the north exposure, with accentuated differences close to saturation (zero pressure head). These differences may have been attributed to differences in texture and organic matter contents observed for the two exposures. Furthermore, $K(\psi)$ presented a tendency to increase with increasing slope. This tendency, observed also in complementary laboratory works was to a part explained by the deviation from requirements of measurements on level ground. A way of adjusting for slope influence is proposed. In the field study, after adjustment, the differences in $K(\psi)$ were attributed to the differences in the vertical and lateral hydraulic conductivity and to the development of surface sealing occurring in low slope plots. Finally, a stepwise regression analysis showed that $K(\psi)$ parameters were explained by the slope of the hillside and the proportion of textural separates in the soil surface.

Key words : tension infiltrometer, rainfed hillsides, slope/exposure, saturated hydraulic conductivity.

Author's address: Manuel Casanova P. Universidad de Chile, Facultad de Ciencias Agrarias y Forestales, Departamento de Ingeniería y Suelos. Casilla 1.004. Santiago, Chile.

Resumen

El tensioinfiltrómetro es un instrumento que permite medir conductividad hidráulica a contenidos de aguas cercanos a la saturación [$K(\psi)$] y en los poros de mayor tamaño del suelo. Regulando la carga de succión durante la infiltración, con la ayuda de una torre de burbujeo, es posible controlar el tamaño de poros que transmite agua. Esta técnica, se utilizó en la caracterización de la infiltración de dos laderas de secano (con exposición norte y sur) de la zona central de Chile. Los resultados mostraron valores inferiores de $K(\psi)$ para la ladera de exposición norte con diferencias acentuadas cerca de la saturación (succión cero). Estas diferencias fueron atribuidas a las diferencias en textura y en los contenidos de materia orgánica observadas entre ambas laderas. Además, la $K(\psi)$ presentó una tendencia a incrementar al aumentar la pendiente de la ladera. Esta tendencia, observada también en un experimento complementario de laboratorio, fue en parte explicada por la desviación ocasionada por la pendiente del terreno, considerando los requerimientos de nivel en las mediciones. Se propone una forma de ajustar acorde a la influencia ejercida por la pendiente. En el estudio de campo, después del ajuste realizado, las diferencias en $K(\psi)$ fueron atribuidas a la conductividad hidráulica vertical y lateral, además al desarrollo de sellamiento en los tratamientos con pendiente reducida. Finalmente, un análisis de regresión (stepwise) mostró que los valores de $K(\psi)$ son explicados fundamentalmente por la pendiente de la ladera y la proporción de separados texturales en la superficie del suelo.

Palabras claves: tensioinfiltrómetro, laderas de secano, pendiente/exposición, conductividad hidráulica saturada.

Acknowledgment

This work was made possible by the support of various persons and two institutions, but I would like to express initially my special thanks to my supervisors, Mr. Abraham Joel and Dr. Ingmar Messing for valuable advice and suggestions.

My special thanks to Dr. Harry Linnér, Head of the Department of Soil Sciences (Division of Agricultural Hydrotechnics) at the Swedish University of Agriculture Sciences, for his friendly hospitality.

I wish to thank everyone at the Department of Soil and Engineering, Agriculture and Forestry Faculty in University of Chile, who has in one way or another, has contributed to the success of this work, especially Alex Rodriguez and my colleagues Mr. Oscar Seguel and Mr. Ian Homer for help in field works, Mr. Walter Luzio and Mr. Wilfredo Vera that replaced me during my academic activities.

Finally, I affectionately dedicate this MSc thesis to my wife Isabel and to my son Manuelito.

1. INTRODUCTION

Large areas in Chile are degraded and have physical and chemical soil constraints. Approximately 94% of the country have limitations for agriculture. The resource degradation is to a large extent caused by the climatic conditions. The arid and semi-arid regimes represent 50% and 32%, respectively, of the total degraded area.

The accelerated soil erosion in Chile began in the 16th century. Both colonists and farmers used fire in uncontrolled way for clearing land. As a consequence, bare steep land subjected to degradation resulted in marginal productivity and fragile agricultural systems for livelihoods of the following generations. Deforestation, over-grazing, over-exploitation and degrading agricultural activities have continued also in the 20th century.

In the Central Zone of Chile, the plant productivity is low because of the brevity of the growth period and the reduced soil water availability. The rainfall regime presents high variability between years, in terms of amounts and seasonal distribution, with isolated events of elevated amounts. These features are characteristic for a climatic type which gives rise to high potential water and sediment runoff, especially when the soils are bare.

For the conditions occurring in semi-arid rainfed zones, little has been published concerning the soil surface hydraulic relationships of hillslope topography. In these zones, the local rainfall is generally the only economically feasible source of water available for crop production. The surface runoff rate is the difference between the rainfall intensity and the infiltration rate of the soil. Therefore the two major determinants of surface runoff rates are the rain characteristics and the infiltration behaviour of the soil.

The quantity and the intensity of the rainfall cannot be controlled by farmers, but they can manage the land to improve the water infiltration capacity in their soils. Therefore, it is very important to characterize the infiltration properties in different conditions of this fragile ecosystem.

2. SCOPE OF WORK

The planning of the work in the present report was done in cooperation between the Department of Soil and Engineering, Faculty of Agricultural and Forest Sciences of the Universidad de Chile, and the Department of Soil Sciences of the Swedish University of Agricultural Sciences in Uppsala. The work was carried out during 1996 and 1997.

2.1 Objective

The objective of the work was to determine soil water infiltration characteristics by means of tension infiltrometer at a site in the inner rainfed area of the central zone of Chile. The measurements were carried out on different gradients on a north and a south slope of an alluvio-colluvial soil.

3. THEORY

3.1 Infiltration theory

Infiltration is the process of water entry into the soil through the ground surface, generally by downward flow through all or part of the soil surface. The maximum rate at which water soaks into, or is absorbed by the soil is termed infiltration capacity or infiltration rate or infiltration velocity. This property is one of the most important processes in the hydrological cycle. Infiltrability is the infiltration flux resulting when water at atmospheric pressure is made freely available at the soil surface (Hillel, 1982).

According to Smith (1972) and Gang Li *et al.* (1995), the rainfall infiltration may be divided into three stages or phases: i) the initial wet-up stage or *non-ponded infiltration*, when the infiltration rate is greater or equal to the rainfall intensity (unsaturated flow), ii) the infiltration declining stage or *pre-ponded infiltration*, when the surface soil becomes saturated, ponding begins to take place on the soil surface and the infiltration rate decreases with the increase in soil water content, iii) the final steady state or *rain-ponded infiltration* when infiltration reaches its final infiltration rate.

The infiltration rate ($q, L T^{-1}$) is determined by the product of the total hydraulic head gradient of the infiltrating water (H/z) and the hydraulic conductivity ($K, L T^{-1}$) of the soil:

$$q = K (H/z) \quad [1]$$

where H is the total hydraulic head (L), and z is the wetted distance (L). The total hydraulic head is the sum of i) a capillary term induced by suction of the field soil, ii) a gravity term induced by the gravity field and, iii) a positive pressure head term induced by ponded water.

When the soil conducts water, the whole pore space is principally involved only when the soil is saturated. As the degree of saturation decreases, the larger pores empty of water and become non-conducting. With flow confined to the smaller pores, moreover to less of the pore space, hydraulic conductivity decreases (Marshall & Holmes, 1992). In field, the largest pores (macropores) can rapidly transport considerable volumes of water to deeper levels during intense or long-lasting rain events (Thomas & Phillips, 1974).

The hydraulic conductivity of a saturated soil (K_{fs}) of stable structure is in principal constant, since the whole of the pore space is assumed water filled. The suffix *fs* however, stands for field-saturated and indicates possible occurrence of pores with entrapped air or other feature that are difficult to control under field conditions. In unsaturated conditions, the hydraulic conductivity [$K(\psi)$] is likely to change in response to the changes in soil water pressure head (ψ), and these changes imply changes in water content (Figure 1). In swelling and shrinking soils, K_{fs} and $K(\psi)$ are affected also by changes in pore space following wetting/drying cycles, and aggregate stability.

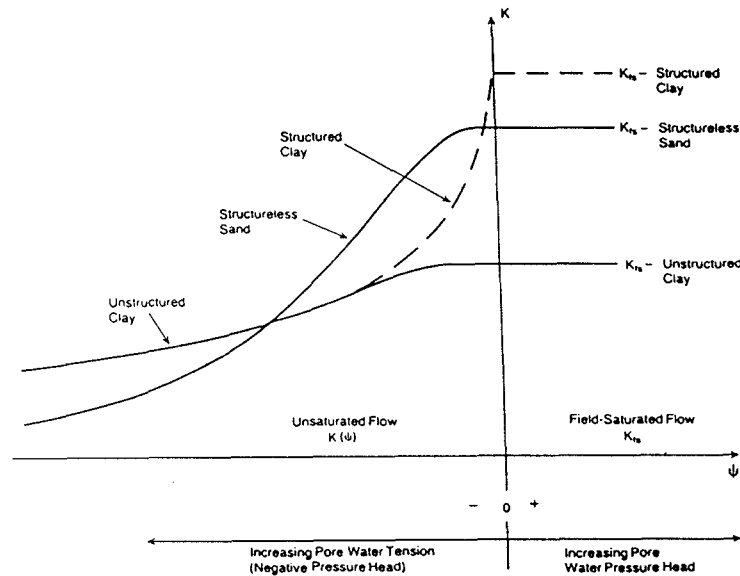


Figure 1. Interactions between hydraulic conductivity [K_{fs} and $K(\psi)$], texture and structure of (Reynolds, 1993).

Most of the processes involving water flow and soil-water interactions in the field above the water table occur under unsaturated conditions (Hillel, 1982; Reynolds, 1993). Thus, $K(\psi)$ and its variation with time and space is very important when predicting how much of the water that arrives at the soil surface will infiltrate into the soil, and how much will flow off overland and potentially causing floods and erosion.

3.2 Factors affecting infiltration rate

According to the Beven & Germann (1982), the porosity can be classified into micropores and macropores. The effect of capillarity within the macropore region is negligible and gravity is the principal driving force for water flow. This bimodal analysis of porosity allows a distinction between slow and fast flowing processes within the soil. Although the fraction of macropore volume is small compared to the total pore volume, macropores are capable of conducting a significant water volume due to their high transport capacity. For some soils, with small matrix K or under specific surface sealing conditions such as crusting or compaction, a large part of the infiltration water may pass through the macropores into deeper soil layers, bypassing the matrix close to the soil surface. In this sense, the total infiltration rate is considered to be the sum of the actual rate into the micropore system (or soil matrix) and the actual rate into the macropore system (Bronstert & Plate, 1997).

Topography greatly influences the microclimate of the soil (Mahler *et al.*, 1979). The amount of water retained is determined by landscape position and slope aspects, for example in fine textured soils often found in the lower parts of slopes that have low intake rates and high runoff potential. It is well known that water may move vertically and/or laterally through the hillslope. Furthermore, the influence of slope aspect and land use dominate the spatial distribution of the infiltration pattern within the basin (Cerdà, 1997).

According to Sullivan *et al.* (1996) the effect of slope on infiltration-runoff is related to the travel time of overland flow. Considering the Manning equation (Manning, 1891), travel time is inversely proportional to the square-root of the slope and proportional to the roughness (Manning's n) and the length of the overland flow path. Thus, for similar surface conditions, a

smaller slope will increase the time for precipitation to travel from the point of impact to a channel and increase the chance of it to infiltrate (or evaporate) downslope before it reaches the channel. Results obtained by Gang Li *et al.* (1995) from moderately tilled slope land showed a decrease in final infiltration rate with increase in slope angle.

In the analysis of Warrick *et al.* (1997) the pressure distributions which develop for steady-state flow through sloping strata were nearly the same as for non-sloping strata, the difference being that the vertical component of the normal direction replaced the vertical coordinate. The major effect of the slope is to deflect flow away from the vertical direction near boundary interfaces. The amount of water deflected horizontally is proportional to the tangent of the slope angle of the strata interface. Therefore, if the slope is small, there is little deflection, but as the slope increases the amount can become substantial.

Luk *et al.* (1993) showed that the development of surface sealing varied with slope gradient. Infiltration was significantly reduced on gentle slope ($< 10^\circ$) due to preferential development of surface crusting and sealing. This result, when compared with data from Gang Li *et al.* (1995), suggests that for gentle slopes, the inverse relation between slope gradient and infiltration under non-crusting conditions, may be reversed under crusted conditions

Ritsema *et al.* (1996) informed in a review that the rate of downhill-directed water flow is not only determined by differences in vertical K between the diagnostic soils horizons, but may also depend on the vertical and lateral K of the soils horizons themselves. Only an extremely high constant anisotropy ratio will cause significant lateral downslope flow during wetting and, a homogeneous isotropic hillslope will not exhibit lateral downslope flow during wetting, but will do so during drying (Jackson, 1992; Philip, 1991).

Hanna *et al.* (1982) found in Southeast Nebraska that the available water content was usually higher in soils on the north-facing slope than in soils on the south-facing slope. The distribution of infiltration rates in the work of Cerdà (1996) showed a clear pattern along the north-facing slope and south-facing slope in Southeast Spain, with the north-facing slope displaying high infiltration rates, while south-facing slope had low infiltration rates (Cerdà, 1997). It should be noted that both cases were in the northern hemisphere. In the southern hemisphere, the reverse should be found.

3.3 Characteristics of tension infiltrometers

The infiltration rate of a soil has been measured by different methods, for example ring or double ring infiltrometer, or a system of 'twing-rings' (McLaren & Cameron, 1996). In order to get field related $K(\psi)$ which can be used in the infiltration theory application, the disc permeameter, also called tension infiltrometer, has been developed (Perroux & White, 1988). Even though designed to measure the increase in air pressure during flood or border irrigation, tension infiltrometers have become widely used standard devices for determining *in situ* hydraulic properties of soils, and have in recent years proved reliable and useful for characterizing soil structural conditions at and near the soil surface. They are portable and relatively non-destructive (when $\psi \leq 0$) and provide simple and inexpensive means to conduct field infiltration tests.

The tension infiltrometer is designed to measure intake at a carefully controlled supply water pressure head, usually from saturation to a few hundred mm of tension, within a circular interface at the soil surface (Figure 6). By maintaining the supply head at a tension, flow into

the larger macropores can be avoided. The flow into the soil profile is unconfined, and infiltration takes place in three dimensions from the circular entrance area.

But as in all fields, there are no panaceas in soil physic. White *et al.* (1992) summarized the many limitations of the tension infiltrometers, which are related principally to simplifying assumptions of the analysis used to extract soil hydraulic properties from water flow measurements. These and other limitations may be:

- Requirement that the soil should be uniform and homogeneous.
- The analysis assumes that the soil is non-swelling.
- Recognition that the determination of steady state conditions requires subjective judgement and patience (specially in heavy textured soils).
- Problem in difficult soils, e.g. hydrophobic soils do not wet up under tension.
- To maintain an intimate contact between the soil surface and the source of water.
- When the measurements are made at supply pressure head close to zero:
 - * infiltrometer must be level, and
 - * the strength of the soil may not be able to support the weight of the device.
- Errors can arise from sampling the volumetric water contents due to :
 - * the small sampling depth required, and
 - * the bulk density of this sample must be known.
- The water reservoirs intercept solar radiation, with a progressive heating and consequently lower viscosities of the water.

The spatial variability of infiltration processes in semi-arid environment is high (Cerdà, 1997). Gang Li *et al.* (1995) marked that, because of the small infiltration area, lateral leakage and the absence of raindrop impact to induce soil surface sealing, the estimated infiltration rates from infiltrometers are considered to be higher than actual rain infiltration rates. The range of $K(\psi)$ that can be measured conveniently with tension infiltrometer is about 10^{-2} to 10^{-6} cm s^{-1} , and the device may not give accurate estimates if the soil is significantly more permeable than the porous disc/membrane and contact material (Reynolds, 1993).

3.4 Tension infiltrometer theory

The analysis of data from tension infiltrometer measurements has rested heavily on several equations (Warrick, 1992). The basic one is an approximation, with a power series, for the early times of infiltration and assumes equivalence to a one-dimensional system (Philip, 1957). The general form of the Philip infiltration model can be expressed as an infinite series in powers, but in practice it is generally sufficient to use an approximate description of infiltration rate ($i, L T^{-1}$) as:

$$\lim_{t \rightarrow 0} (i) = \lim_{t \rightarrow 0} [Q(t) / \pi r^2] = \frac{1}{2} S t^{-1/2} \quad [2]$$

where $Q(t)$ is the flow from the tension infiltrometer ($L^3 T^{-1}$), r is the disc radius (L), and S is an unsaturated soil coefficient called sorptivity ($L T^{1/2}$), that is an integral measure of soil capillarity (Philip, 1969) or an integral property of the soil water diffusivity (White & Perroux, 1987). According to Mwendera & Feyen (1993), S indicates the initial capacity of the soil to absorb water, without reference to gravitational effects (Philip, 1957), and is a function of the initial soil water content.

The integration of equation 2 with respect to time results in the cumulative intake per unit area (I , $L^3 L^{-2}$):

$$\int_0^t i \, dt = I = S t^{1/2} \quad [3]$$

indicating that at small time increments, the intake of water proceeds as $t^{1/2}$ (just as in horizontal infiltration)

Figure 2 shows graphically I versus t for two regions. Region I is before steady state flow, and region II is where steady state flow has been reached (Cook & Broeren, 1994). The determination of the steady state infiltration flow (Q_∞ , $L^3 T^{-1}$) is calculated from the slope of I versus t in region II.

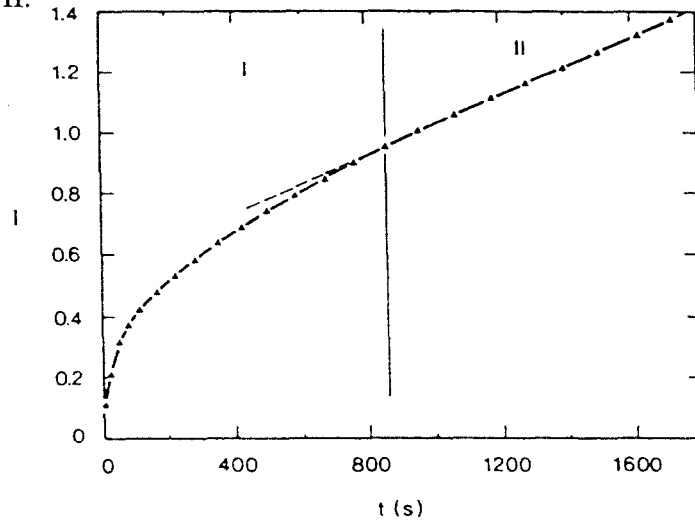


Figure 2. Cumulative infiltration (I) versus time (t) (Cook & Broeren, 1994).

Figure 3 represents I plotted against $t^{1/2}$ but in terms of three regions, relating to the infiltration pattern under a tension infiltrometer. Region I is due to contact material (sand) sorption, region II is due to sorption of the soil, and region III is where the flux is tending toward steady-state (Cook & Broeren, 1994; Cook *et al.*, 1993). S is simply the slope of I versus $t^{1/2}$ in region II.

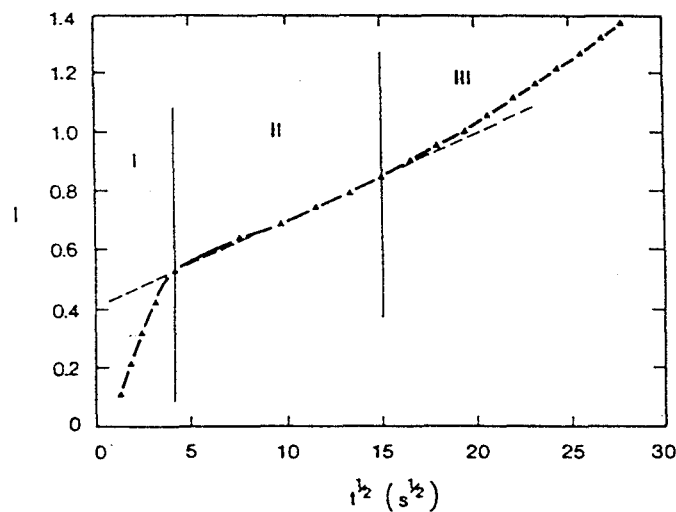


Figure 3. Cumulative infiltration (I) versus $t^{1/2}$ (Cook & Broeren, 1994).

The other commonly used relationship is the approximate, but usefully accurate, solution for flow from a circular pond at steady state conditions found by Wooding (1968). This linearized solution uses a hydraulic conductivity function (Gardner, 1958):

$$K = K_{fs} \exp(\alpha \psi) \quad [4]$$

where α is the exponential slope (L^{-1}) equivalent to λ_c^{-1} (λ_c , is the macroscopic capillary length scale) and ψ is the soil water pressure head (L). Wooding (1968) showed that the steady state rate from a circular source can be approximated as:

$$Q_{\infty} / \pi r^2 = q = \Delta K [1 + (4 \lambda_c / \pi r)] \quad [5]$$

where q is the steady state infiltration rate ($L T^{-1}$), ΔK is the difference between K values at the supply pressure head $K(\psi_o)$ and the initial soil water pressure head $K(\psi_n)$.

Assuming (Ankeny *et al.*, 1991) that K ahead of the wetting front at ψ_n is much smaller than $K(\psi_o)$:

$$q = K(\psi_o) [1 + (4 / \pi r \alpha)] \quad [6]$$

and applying eqs. 4 to 6 piece-wise such that α is constant between consecutive supply pressure heads (ψ_i and ψ_{i+1}) (Reynolds & Elrick, 1991):

$$\alpha_{i+1/2} = [\ln (q_i / q_{i+1/2})] / (\psi_i - \psi_{i+1/2}); \quad i = 1, \dots, n-1 \quad [7]$$

where n is the number of supply pressure heads used (Figure 4).

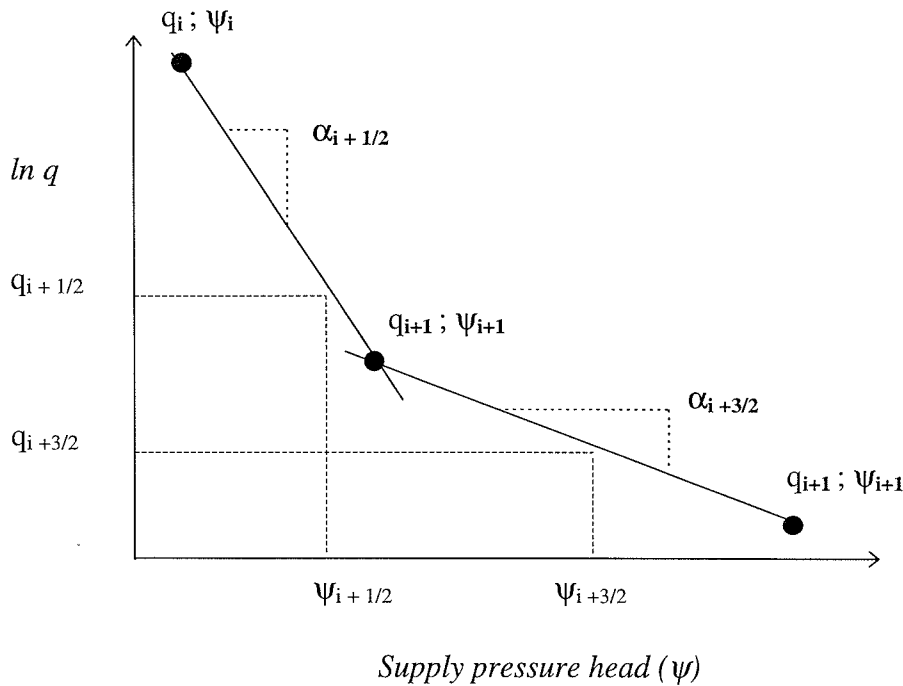


Figure 4. Piece-wise estimation of $q(\psi)$ and α (Messing, 1993).

Combining equations 6 and 7 give :

$$K_{i+1/2} = q_{i+1/2} / [1 + (4 / \pi r \alpha_{i+1/2})]; \quad i = 1, \dots, n-1 \quad [8]$$

where the steady-state infiltration rates at the midway points between adjacent supply potentials $(\psi_i + \psi_{i+1})/2$ are assumed to be given by :

$$q_{i+1/2} = \exp \{ [\ln (q_i) + \ln (q_{i+1})] / 2 \}; \quad i = 1, \dots, n-1 \quad [9]$$

The $K(\psi)$ values are determined from infiltration rate data according to eq. 8. Since $K(\psi)$ relations are generally exponential over only small ranges, the accuracy of the $K(\psi)$ values tends to increase with the number of supply pressure heads used. It is recommended that three to five supply pressure head increments be used to provide adequate definition of the near-saturated relationship (Reynolds, 1993).

4. MATERIALS AND METHODS

The experimental work principally considered a field work in Chile at the Germán Greve Silva Experimental Station (E. S.), approximately 20 km from Santiago and a complementary laboratory work at Ultuna in Sweden.

4.1 Field work (Chile)

4.1.1 Physiography

Chile consists of three different longitudinal structural zones: a) the range of high mountains (*Cordillera de Los Andes*), b) the coastal range (*Cordillera de la Costa*) and c) the Central Valley. Furthermore a series of insular, latitudinal and altitudinal climatic zones.

Santiago city is located at the northern end of Chile's central intermont basin, extending from the foot of *Los Andes* toward the coastal range at an altitude of 550-600 m. The older and central part of the city was built on both sides of a small river, the Mapocho (a tributary of the Maipo, one of Chile's largest rivers). Snow-capped peaks of *Los Andes*, reaching altitudes of over 6,000 m, rise above the city. Some of these peaks are extinct, truncated, cone-shaped volcanoes. An important feature is the existence of wide alluvial valleys, with plane and wide bottom. (Brüggen, 1950).

The coastal range (*Cordillera de la Costa*) follows the coastline closely throughout northern and central Chile. It rises abruptly from the shoreline in high cliffs that for hundreds of km form an unbroken wall, creating a coastline devoid of natural harbours and an obstacle to access inland. Large parts of the coastal range are actually an eroded plateau descending west to the sea by cliff-bound terraces. The coastal range rises to an altitude of approximately 2,700 m.

The coastal range is the west boundary of the Santiago basin. Börgel (1966) pointed out that the central depression corresponds to two fault lines forming a sinking grave with two evident lines of tectonic fractures (see 4.1.3). The hillside evolution shows a pattern with incipient development and strong gradient, colonized by steppe vegetation.

4.1.2 Location

The studied zone is inserted in the east-side of the coastal range, in particular known as *Inner Rainfed*. The study area was located (Figure 5) in a microbasin of the Germán Greve Silva E.S. in the rainfed area of Ovine Research Program which belongs to the Husbandry Department of the Agricultural and Forestry Faculty of Universidad de Chile: approximately 7 km to the south of Maipú's commune, and 25 km to the west of Santiago city, Chile (33° 28' South -70° 50' West) at 470 m above sea level. The Germán Greve Silva E.S. includes 2,940 ha, with 206 ha irrigated with security, 1,210 ha irrigated with contingency (pumping), and with a rainfed area including a plain zone of 40 ha and a hilly zone of 1,484 ha.

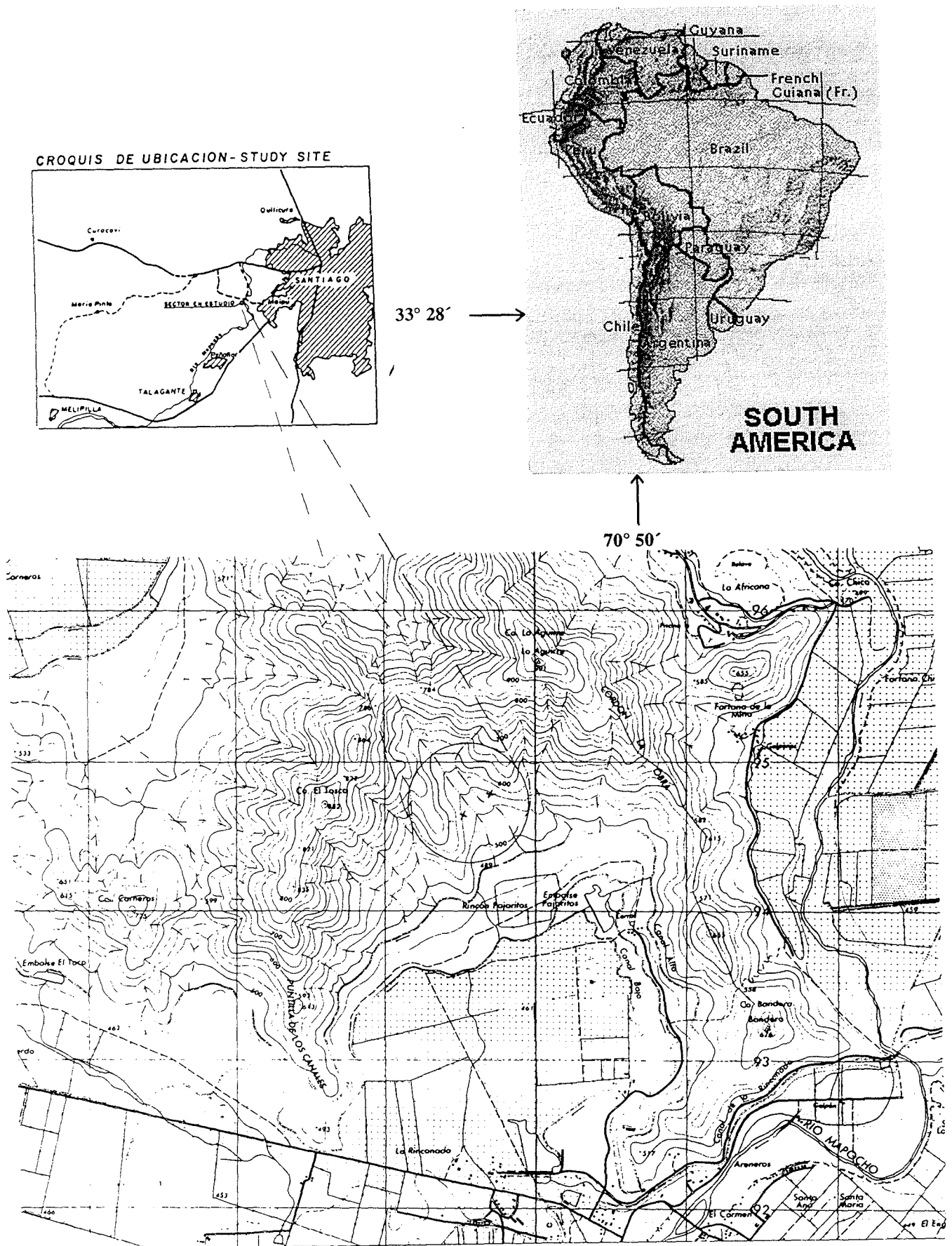


Figure 5. Location of the two sites: north-facing slope and south-facing slope (marked with X).

4.1.3 Geology and geomorphology

The physical structure of South America with its major surface features (mountain systems, plateaus, river basins and plains) is the product of a complex of successive geological processes. Endogenic and exogenic forces continuously at work over the long geological history of the continent, caused many drastic changes in its shape and relief leading to its present surface and structural characteristics.

The geological processes that led to the creation of *Los Andes* began when the Andean Geosyncline (a large linear trough along the margin of a continent) extended along what is now the entire western and part of the northern coast of the continent. There are indications that movements of the earth's crust leading to the rise of *Los Andes* were active during the early part of the Mesozoic era. It is assumed that the movements started even earlier. However, they were most forceful during the Middle and Upper Tertiary periods, when the uplifting process of *Los Andes* reached its peak, although it actually continued into the Pleistocene epoch. The sediments of the Andean Geosyncline when uplifted by movements of the earth crust were intensely folded and faulted, thus forming the ranges of *Los Andes*.

This mountain-building process, accompanied by large intrusions of igneous rock and much volcanic activity, formed some of the thickest formations of volcanic materials on the earth (in Peru and Chile). *Los Andes* assumed most of their present form toward the end of the Tertiary period, when they were already the continuous formidable wall along the entire western fringe of the continent. One of the last major events affecting the continental surface was the extensive glaciation during the Pleistocene epoch, when glaciers covered much of the *Los Andes* from the extreme south.

According to Chile-Comisión Nacional de Riego (1981), the rocks in the study area are principally igneous volcanic as well as intrusive, and from Mesozoic Age. The coastal range is constituted of granite rocks defined as coastal granodioritic batholit. The quaternary processes of the Santiago basin presents two particularities, its considerable thickness and its variety of sediments, which are consequences of basin specific conditions by interaction of tectonic, climatic oscillations and volcanic influences.

The soils in the study area occur on a lightly inclined plain and rest above colluvial substratum (gravels and stones), and have a sandy clay loam matrix, at a depth of 1 - 100 cm. The parent material is mixed and principally porphyritic.

4.1.4 Climate

The general climate in the study area is classified according Köeppen climatic classes as Warm Temperate with extended dry season (6 to 8 months), corresponding to Csb1: temperate climate zone, with dry and warm summer, winter rainfalls, annual thermal amplitude higher than 10°C and annual mean precipitation of approximately 270 mm. It is characterised by a strong seasonal rainfall distribution, with 75% falling in the winter months (see Appendix 1 : *Climate*).

4.1.5 Vegetation

The study area presents a degraded natural prairie, periodically grazed by ovine. Nevertheless, dominant vegetation formation is named as “espinal”, also named *Acacia cavens* steppe. This is a common natural ecosystem in the central zone of Chile, generally observed as thorny trees and shrubs with a spring-time grass cover rich in annual plants. Other species in the rainfed zone are Trebo (*Trevoa trinervis*), Quillay (*Quillaja saponaria*), Palqui (*Cestrum parqui*), Guayacán (*Porliera chilensis*) and *Nasella*, *Bromus*, *Verbena*, *Calceolaria*, *Galium* y *Oxalis* genus species.

4.1.6 Study sites and treatments

The site was chosen due to its uniformity according to the topographic survey of the area carried out at scale 1:2.000 in January, 1996 (see Appendix 2: *Topographic survey*). The soil belongs to the *Piedmont Cuesta de Barriga* soil series according to Chilean soil survey (Chile-Comisión Nacional de Riego, 1981) (see Appendix 3: *Soil description*).

The soil is an inceptisol of alluvio-colluvial origin and moderately deep. The profile with north exposure presented a horizon sequence: A-Bw-BC-C-IIC, and the south exposure soil: A-Bt. It had a vegetation of savanna with a degraded prairie, thermic soil temperature regime (average annual temperature: 14.2°C) and xeric soil moisture regime. The soils were well drained with a moderately slow and rapid, internal and external drainage, respectively.

In the rainfed area under study, the high and medium slope of hillsides are affected by degradation (sheet erosion). The low slopes are affected by deposition processes, especially on the north-facing soils. The south-facing hillside showed features of landslides, possibly increased by the tunnel making activities of *Octodon degú*, a common vegetarian cavimorph rodent in the rainfed zone of Chile.

Measurements with tension infiltrometers were conducted on eighteen 2 m² (2 x 1m) micro-catchments constructed on six different slope gradients. Nine of the plots had north exposure and nine had south exposures. The treatments were named :

NL1	NM1	NH1	SL1	SM1	SH1
NL2	NM2	NH2	SL2	SM2	SH2
NL3	NM3	NH3	SL3	SM3	SH3

where N/S corresponds to aspect (north and south exposure), L/M/H to slope (low, medium and high gradient) and 1/2/3 represent the repetitions. One sample (NH3) gave erratic values and was not used in the analysis.

The study was carried out during the spring season October to December in 1996. It is of general knowledge that the infiltration rates increase from spring to summer and decrease from summer to autumn, reaching the maximum in late summer. Therefore, the measurements in this study were made in spring/summer, a dry and hot period characterized by higher infiltration rates in both natural semi-arid areas and in agricultural fields.

In each plot, the soil nearby the location of measurements was sampled in triplicate at the depth of 0 - 2 cm for gravimetric determination of initial water content. The samples were dried 24 hours in 105°C.

Two tension infiltrometers (Figure 6) with disc radii of 100 mm were used in the determination of infiltration characteristics of the surface soil (CSIRO, 1988). The reservoir of the infiltrometer was filled with distilled water to avoid differences in water quality between seasons and because semi-arid soils are influenced by the chemical composition of the rain (Shainberg *et al.*, 1981; Agassi *et al.*, 1994; Kim and Miller, 1996).

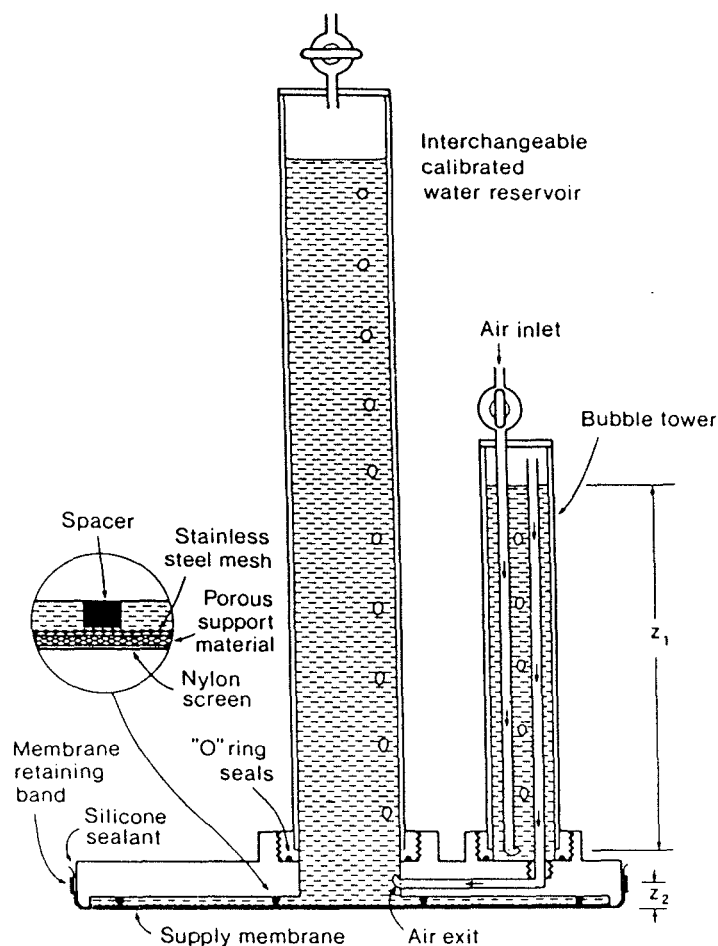


Figure 6. Disc permeameter used for unsaturated measurements (CSIRO, 1988).

Any outstanding surface irregularities were removed with a knife. A thin layer of moist fine sand was applied over the soil surface in a circular area of approximately the same diameter as the infiltrometer disc, to ensure a good contact and a uniform hydraulic link between the uneven soil surface and the flat, rigid porous base of the tension infiltrometer (Messing & Jarvis, 1993). The porous base plate was placed on the prepared sand surface in each micro-catchment and infiltration test was run in sequence at the same position, to reduce effects of spatial variability (Logsdon & Jaynes, 1993), at -10, -6, -4, -2 and -1 cm supply water pressure heads by adjusting the elevation of the air tube in the bubble tower. To achieve steady state conditions, the infiltration tests were run 35, 30, 25, 25 and 25 min, respectively.

The rate of water flow out of the infiltrometer and into the soil was measured by monitoring the rate of fall of the water level on the reservoir measurement scale, with manual recording at 30 seconds time intervals.

As a precaution against changes in water viscosity caused by sunlight heating of the supply reservoir, the device was kept shaded with a screen during measurements.

Each sequence of infiltration runs at a given location started with the smallest supply pressure head, increasing stepwise to the largest pressure head. That is to minimize the hysteresis effect encountered by a wetting front expanding beyond that of the last measurement if a decreasing sequence of supply pressure heads was applied (Cook & Broeren, 1994; Messing & Jarvis, 1993; Reynolds & Elrick, 1991).

Immediately at the end of each infiltration sequence, the disc was removed from the soil surface, the sand scraped away, and when the free water disappears from the surface, soil was sampled to a depth of 0-1 cm for gravimetric determination of the final water content, i.e. the water content at -1 cm pressure head. This was subsequently converted to volume basis using bulk densities determined on cores, sampled after infiltration measurements in each micro-catchment (Blake & Hartge, 1986a). Furthermore, samples were taken for particle size distribution using Bouyoucos's hydrometer method (Gee & Baude, 1986). Particle density was determined by means of picnometer method (Blake & Hartge, 1986b). Particle density and dry bulk density were used in the estimation of total porosity in each sample. The organic matter content was estimated utilizing Walkley and Black method (Black, 1965). Finally, the slope gradient in each plot was measured with engineer level.

4.2 Laboratory work (Ultuna - Sweden)

This complementary work consisted in analyzing the interaction between infiltration rate and slope gradient. The purpose was to eliminate the effects of texture and soil surface crusting or sealing, which varied in field with the slope gradient.

4.2.1 Soil

The soil used came from Nântuna and was described by Linnér (1984) as a low humus loamy sand soil. Table 1 includes particle size distribution and organic matter content (O.M) of the soil.

Table 1. Characteristics of Nântuna soil (Linnér, 1984)

Particle diameter (mm):	< 0.002	0.002 - 0.02	0.02 - 0.2	0.2 - 2.0	> 2.0	O.M.
(%) :	8	5	18	68	0	1

4.2.2 Treatments

Infiltration tests were conducted on nine 0.066 m³ (0.550 x 0.375 x 0.320 m) plastic boxes disposed at three different slope gradients: three boxes with 0%, three with 12.5% and three with 25% slope gradient. All boxes were treated in an identical way; filled 10 cm at the time

to 35 cm height and shaken 15 seconds at each fill in order to consolidate the soil and reduce variability among the boxes. The treatments were named :

NÅZ1	NÅM1	NÅH1
NÅZ2	NÅM2	NÅH2
NÅZ3	NÅM3	NÅH3

where Z/M/H correspond to slope gradient (zero, medium and high gradient) and 1/2/3 represent the repetitions. The infiltration tests were run as in the field, i.e. at the same position at -10, -6, -4, -2 and -1 cm supply water pressure heads, during 35, 30, 25, 20 and 16.5 min, respectively.

4.3 Treatment of the data

Following the methodology of Messing & Jarvis (1993) based on a solution for infiltration from a circular source (Wooding, 1968), paired (K, ψ) values were obtained from steady-state infiltration rates at successive supply pressure heads (see section 3.4). All paired (K, ψ) data obtained for the three repetitions at each gradient and aspect were summarized with two linear regression models, line one for data > -4 cm pressure head and line two for the data ≤ -4 cm pressure head. It is assumed that an exponential $K(\psi)$ function can be applied in two pore systems with a division at a boundary pressure head ψ_b between macropores and mesopores (Keng & Lin, 1982; Messing & Jarvis, 1993) so that:

$$\ln K = \ln K_{fs} + \alpha_1 \psi \quad \psi > \psi_b \quad [9]$$

$$\ln K = \ln K_o + \alpha_2 \psi \quad \psi < \psi_b \quad [10]$$

where α_1 and α_2 are the semi-log slopes of the regression lines, and K_{fs} and K_o are estimated by extrapolating to zero pressure head. The prolongation of the lines outside the boundary ranges in figures 9, 10 and 14, are retained only for clearness of the procedure used.

An analysis of stepwise regression was carried out with STATGRAPHIC program with the goal of obtaining a small set of variables significant for $\ln K_{fs}$, $\ln K_b$ and ψ_b . The parameters used in this analysis are included in Table 2.

5. RESULTS AND DISCUSSION

Soil water is a crucial factor in the growth and development of plants in arid and semi-arid environments and as a consequence, controls the behaviour of the ecosystem. Therefore, due to their interactions with other factors, infiltration processes could be considered a synthetic ecological factor.

5.1 Field work results

As shown in Table 2, the textural class of the surface horizon in all the plots studied was loamy (U.S.D.A. Classification system), but with higher clay contents in south-facing soils (15.2% to 26.9%) than in north-facing soils (12.9% to 18.5%). The soil organic matter contents had a tendency to be smaller in the north facing soils (2.7% to 7.8%) than in the south-facing (6.4% to 11.2%).

The slope gradients varied between averages of 13.3% (low), 20.5% (medium) and 27.7% (high) for the north exposure, and between averages of 12.1% (low), 15.4% (medium) and 24.9% (high) for the south exposure.

Table 2. Soil surface characteristics measured in the 18 sites

Site	W_i ($g\ g^{-1}$)	W_f ($g\ g^{-1}$)	Db ($Mg\ m^{-3}$)	Dp ($Mg\ m^{-3}$)	Clay (%)	Silt (%)	Sand (%)	O. M. (%)	Slope (%)
NL1	0.030	0.440	1.39	2.67	13.2	38.3	48.5	7.78	13.7
NL2	0.028	0.380	1.51	2.47	15.3	36.0	48.7	7.09	10.2
NL3	0.017	0.361	1.42	2.68	15.2	39.9	44.9	5.85	15.7
NM1	0.017	0.336	1.57	2.74	14.7	35.0	50.3	6.74	20.9
NM2	0.019	0.305	1.53	2.34	12.9	36.9	50.2	6.89	20.0
NM3	0.018	0.347	1.68	2.64	13.1	36.7	50.2	6.65	20.7
NH1	0.021	0.377	1.60	2.63	13.3	37.9	48.8	7.73	27.9
NH2	0.022	0.317	1.35	2.71	14.8	38.3	46.9	2.70	28.7
NH3	0.019	0.290	1.64	2.65	18.5	38.9	42.6	5.52	26.4
SL1	0.019	0.483	1.44	2.59	15.2	36.9	47.9	9.17	13.1
SL2	0.020	0.385	1.46	2.59	18.6	33.3	48.1	6.42	11.4
SL3	0.018	0.384	1.43	2.64	26.9	39.6	33.5	6.94	11.9
SM1	0.025	0.462	1.25	2.60	24.2	38.2	37.6	11.15	17.4
SM2	0.021	0.384	1.44	2.62	25.1	38.6	36.3	10.08	14.2
SM3	0.021	0.393	1.38	2.61	23.7	39.1	37.2	8.52	14.6
SH1	0.019	0.379	1.61	2.62	22.5	36.2	41.3	6.53	20.4
SH2	0.016	0.442	1.39	2.68	23.6	35.4	41.0	7.82	26.8
SH3	0.023	0.410	1.23	2.70	25.3	39.5	35.2	6.95	27.6

S	=	south exposure	W_i	=	initial gravimetric water content
N	=	north exposure	W_f	=	final gravimetric water content
L	=	low slope	Dp	=	particle density
M	=	medium slope	Db	=	dry bulk density
H	=	high slope	O.M.	=	organic matter content

In the Table 3, calculated and estimated soil surface characteristics used in the following discussion are presented.

Table 3. Soil surface characteristics calculated or estimated in the 18 sites

Site	$\ln K_{fs}$ (mm h^{-1})	ψ_b (- mm)	$\ln K_b$ (mm h^{-1})	θ_i ($\text{m}^3 \text{m}^{-3}$)	θ_f ($\text{m}^3 \text{m}^{-3}$)	ϕ (%)
NL1	2.612	42.799	0.515	0.0411	0.6115	47.94
NL2	2.227	45.222	0.373	0.0429	0.5732	38.87
NL3	3.260	27.419	0.710	0.0243	0.5123	47.01
NM1	4.114	30.438	1.009	0.0264	0.5277	42.70
NM2	3.914	30.372	1.697	0.0294	0.4673	34.62
NM3	3.567	51.655	0.984	0.0304	0.5825	36.36
NH1	3.555	32.241	2.136	0.0333	0.6032	39.16
NH2	4.490	49.195	0.899	0.0296	0.4277	50.18
NH3	-----	-----	-----	0.0308	0.4761	38.11
SL1	3.717	25.557	1.858	0.0272	0.6957	44.40
SL2	2.187	-----	-----	0.0288	0.5620	43.63
SL3	3.288	38.801	0.688	0.0256	0.5490	45.83
SM1	4.344	42.920	1.254	0.0319	0.5773	51.92
SM2	4.186	34.721	1.999	0.0298	0.5530	45.04
SM3	4.643	43.804	1.226	0.0290	0.5423	47.13
SH1	4.644	65.733	1.686	0.0306	0.6107	38.55
SH2	5.188	48.547	1.450	0.0221	0.6147	48.13
SH3	5.380	33.783	2.480	0.0282	0.5048	54.44

K_{fs} = field saturated hydraulic conductivity

ψ_b = pressure head in the break point

ϕ = porosity : [1 - (Db/Dp) x 100

θ_i = initial volumetric water content

θ_f = final volumetric water content

K_b = unsaturated hydraulic conductivity in the boundary point

As an example, infiltration curves for -10 cm supply water pressure head are presented in figures 7 and 8. Infiltration depths, were highly variable within each exposure. At the end of the measurements (35 min), they had a mean (μ) = 5.58 mm and a standard deviation (σ) = 3.56 mm for the south-facing soils, and μ = 7.40 mm and σ = 3.56 mm for the north-facing soils. Considering that in both exposures the initial volumetric water contents of the soils were very low and similar (means of 2.8 % south and 3.2 % north), the relatively high clay (22.8 % south and 14.6 % north) and organic matter (8.2 % south and 6.3 % north) contents in the south-facing soils may explain the lower sorptivity expressed. The same tendency also applied to the other supply pressure heads.

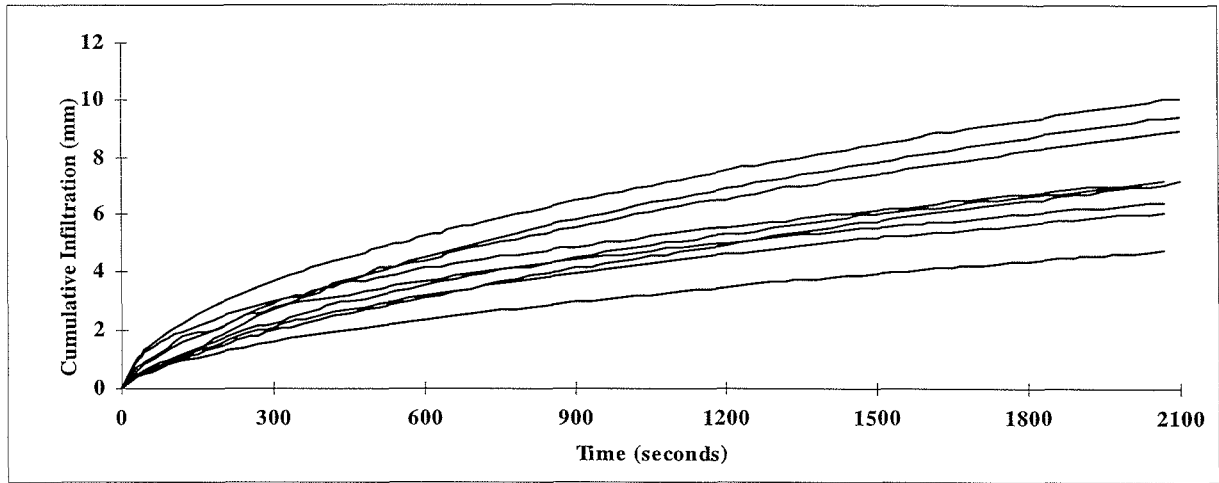


Figure 7. Infiltration depth for 18 plots at the supply pressure head = -10 cm. North facing soils.

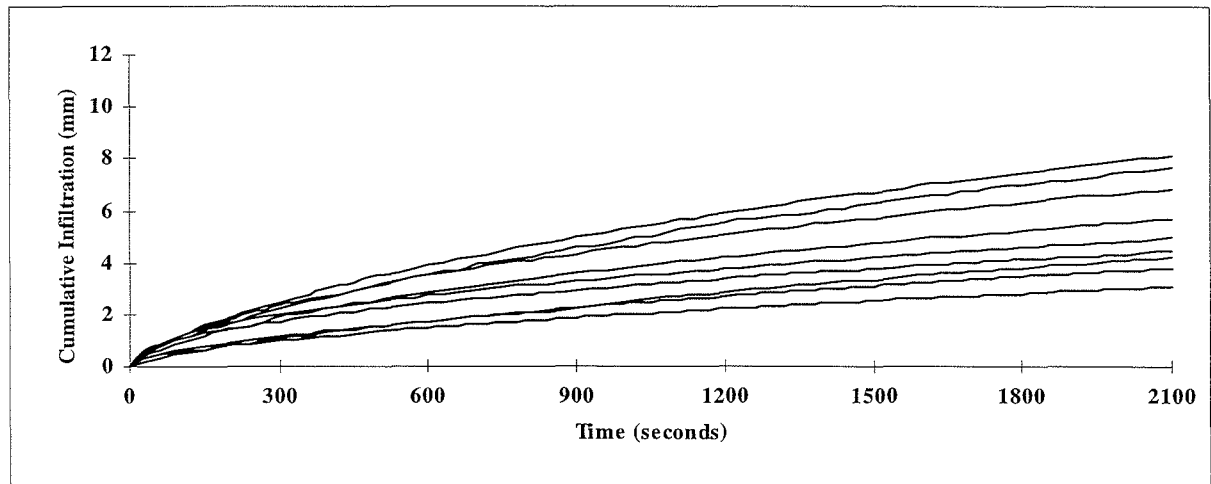


Figure 8. Infiltration depth for 18 plots at the supply pressure head = -10 cm. South facing soils.

Log-transformed hydraulic conductivity (K) for 17 of 18 samples plotted against soil water pressure head (ψ), showed that two-line representation was more appropriate than one linear representation (figures 9 and 10) with a boundary pressure head (ψ_b) between -35.3 mm and -47.8 mm for the soils with north exposure and between -41.6 mm and -49.0 mm for the soils with south exposure.

The hydraulic conductivity $K(\psi)$ of the north-facing locations decreased initially at a rate (α_1) in the order of 0.059 to 0.075 mm^{-1} , while in the south-facing locations this rate varied between 0.052 and 0.069 mm^{-1} .

The R^2 values were generally large for the macropore lines ($0 < \psi < \psi_b$) and intermediate to low for the mesopore lines ($\psi_b < \psi < -100$ mm). This indicates a large variability among repetitions in the mesopore region, due to large spatial variability or to shortcoming in the measurement or calculation procedures.

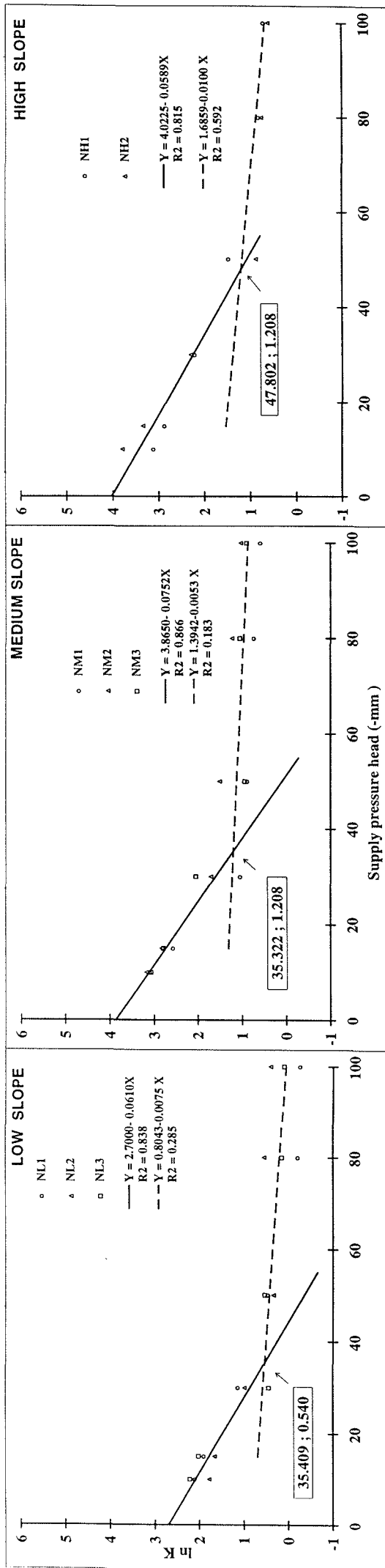


Figure 9. The observed values of the logarithm of hydraulic conductivity (mm h^{-1}); vs. supply pressure head and the estimated two regression lines. North-facing soils.

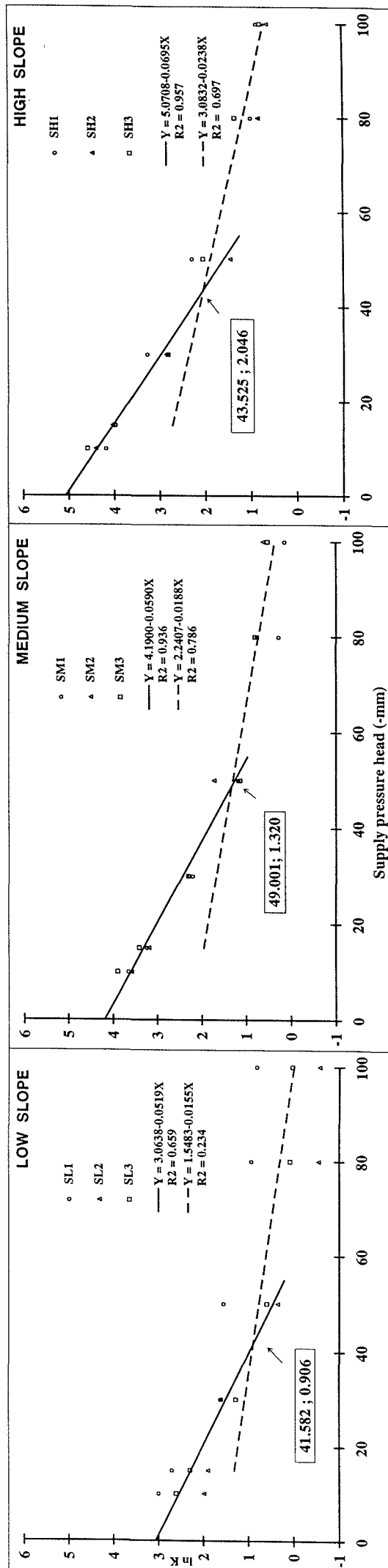


Figure 10. The observed values of the logarithm of hydraulic conductivity (mm h^{-1}); vs. supply pressure head and the estimated two regression lines. South-facing soils.

By superimposing the graphs in Figure 9 and 10 on each other it can be seen (Figure 11) that:

i) Increasing slope gradients gave higher K values in the whole ψ range, approximately one order of magnitude increase between low and medium slope, and half an order of magnitude between medium and high slope. The only exception was the mesopore range in north high slope (NH) which did not have higher K values than at the medium slope.

ii) The northern slopes showed half an order of magnitude lower K values in the macropore region compared to southern slope, a tendency to lower K and α values in the mesopore range.

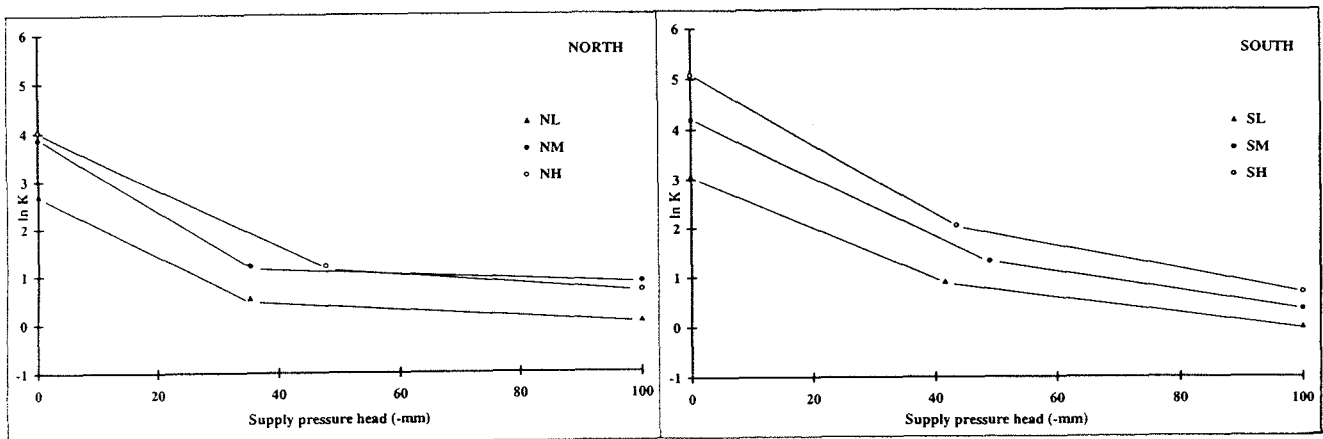


Figure 11. Comparison of regression lines in figures 9 and 10.

Considering K_{fs} for each repetition, estimated by extrapolating to zero supply pressure head, there was a tendency for higher values at higher slope gradients than at lower. This applied to north-facing as well as to south-facing soils, but with higher values in the south-facing soils (figures 12 and 13). This behaviour may be caused by the processes of erosion at higher slope and deposition at the lower slopes. The determination coefficient (R^2) values for the macropore straight lines in these estimations varied between 0.991 and 1.000.

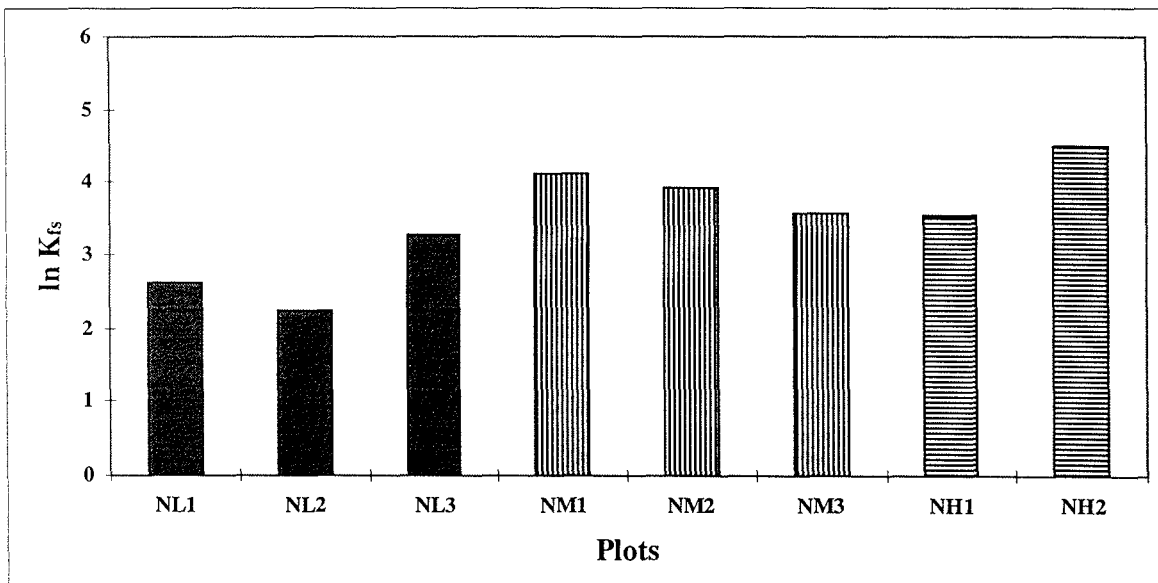


Figure 12. Field saturated hydraulic conductivity (K_{fs} , mm h^{-1}) estimated by extrapolating to zero supply pressure head. Replicates of the north-facing soils.

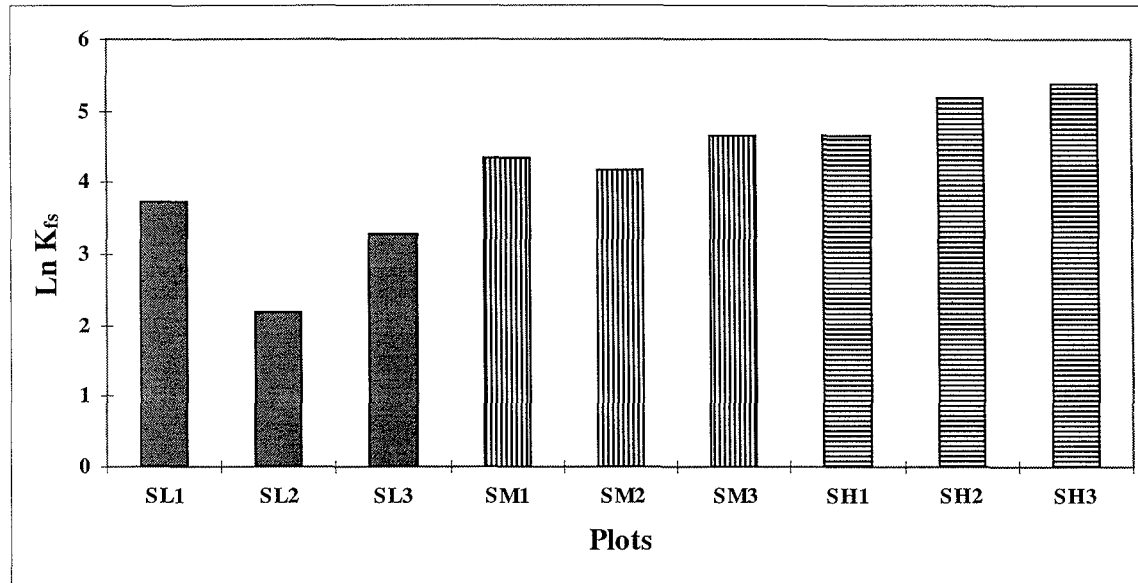


Figure 13. Field saturated hydraulic conductivity (K_{fs} , mm h^{-1}) estimated by extrapolating to zero supply pressure head. Replicates of the south-facing soils.

The stepwise regression analysis showed in the case of the north-facing soils, with $\ln K_{fs}$ (in mm h^{-1}) as dependent variable, clay content (Cl) and slope (m) as the most significant ($P < 0.05$) independent variables of those in Table 2. For the south-facing soils, silt content (Si) and m were most significant ($P < 0.05$). The models obtained were:

North-facing soils:

$$\ln K_{fs} = 0.103 \text{ Cl} + 0.103 \text{ m} \quad R^2 = 0.99$$

South-facing soils:

$$\ln K_{fs} = 0.179 \text{ Si} + 0.130 \text{ m} \quad R^2 = 0.84$$

In a second analysis, with $\ln K_b$ and ψ_b as dependent variables, the models obtained ($P < 0.05$) by stepwise procedure were:

North-facing soils:

$$\begin{aligned} \ln K_b &= 0.048 \text{ m} & R^2 &= 0.91 \\ \psi_b &= 8.378 \theta_i + 0.706 \text{ m} & R^2 &= 0.98 \end{aligned}$$

South-facing soils:

$$\begin{aligned} \ln K_b &= 0.079 \text{ m} & R^2 &= 0.87 \\ \psi_b &= 1.647 \text{ Cl} & R^2 &= 0.86 \end{aligned}$$

These results showed a close relationship between the slope gradient and K_b . Additionally, ψ_b was determined by the initial volumetric water content (north) and clay contents (south).

5.2 Laboratory results

A general trend of higher K values with increasing slope gradient was observed in the field measurements (section 5.1). The laboratory work had the objective to distinguish the effects of slope on the infiltration rate and K_{fs} . In laboratory, conditions were assumed better to reach soil uniformity and homogeneity requirements. Initial water contents varied between 5.5% and 6.6%, and the dry bulk densities between 1.63 Mg m^{-3} and 1.74 Mg m^{-3} (Table 4).

Table 4. Soil surface characteristics measured and estimated in the 9 boxes with Nântuna soil

Box	W_i (g g^{-1})	Db (Mg m^{-3})	$\ln K_{fs}$ (mm h^{-1})	Slope (%)
NÄZ1	0.062	1.66	4.686	0
NÄZ2	0.055	1.74	4.892	0
NÄZ3	0.060	1.70	4.353	0
NÄM1	0.066	1.65	4.619	12.5
NÄM2	0.054	1.68	4.932	12.5
NÄM3	0.058	1.67	4.559	12.5
NÄH1	0.061	1.74	4.598	25.0
NÄH2	0.061	1.63	4.902	25.0
NÄH3	0.059	1.71	4.872	25.0

The laboratory soil had a larger content of sand and a smaller content of clay, silt and organic matter than the field soils (tables 1 and 2). Therefore, the $\ln K - \psi$ regression lines were found at one to two order of magnitudes larger K values in the laboratory study (Figure 14) compared with the field study (figures 9 and 10).

As for the field soils, two-line representations were more appropriate than one line representations (Figure 14) with ψ_b being -45.2 mm , -42.4 mm and -57.1 mm for the samples with zero (0%), medium (12.5%) and high (25%) slope, respectively. The hydraulic conductivity decreased initially (α_1) in the order of 0.038 , 0.043 and 0.033 mm^{-1} , for the respective slope, while in the mesopore system this decrease (α_2) was 0.024 , 0.043 and 0.026 mm^{-1} . In comparison with the field soils, the differences between α_1 and α_2 values were smaller, and thus the bimodal character of the pore system was less developed in the laboratory soil.

Comparing the lines representing different slopes in Figure 14 shows, that they were fairly similar. The high slope line lied a quarter to half and order of magnitude higher than medium and zero slope (Figure 15a).

In the estimated K_{fs} , there was a tendency, although not significant, of decrease from the boxes with high slope to those with zero slope. This tendency was similar to those observed in the field study, but could in the latter case be a response to differences on the vertical and lateral hydraulic conductivity of the soils layers (Ritsema *et al.* 1996).

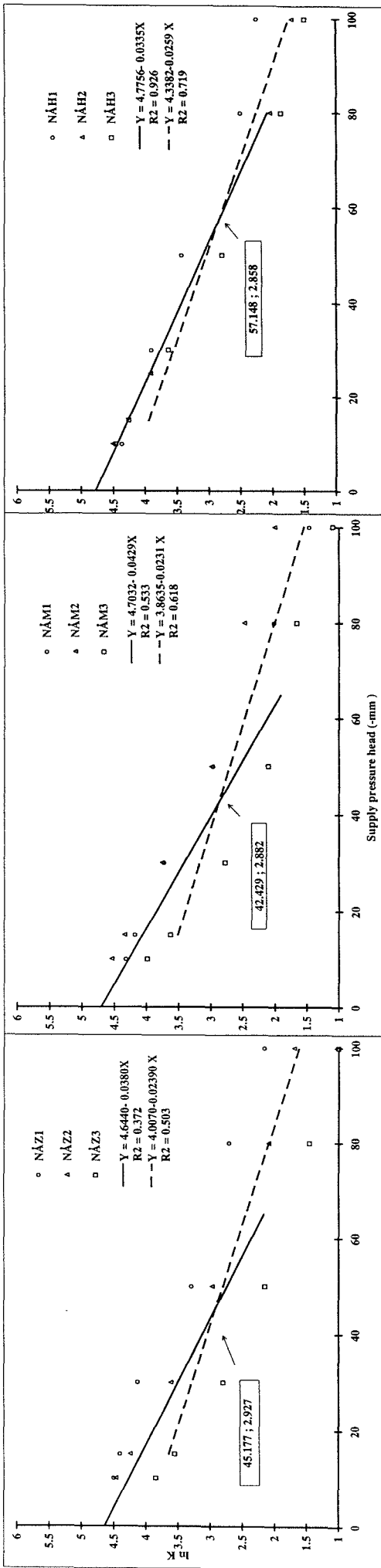


Figure 14. The observed values of the logarithm of hydraulic conductivity (mm h^{-1}), vs. supply pressure head and the estimated two straight lines by slope range. Nántuna soil.

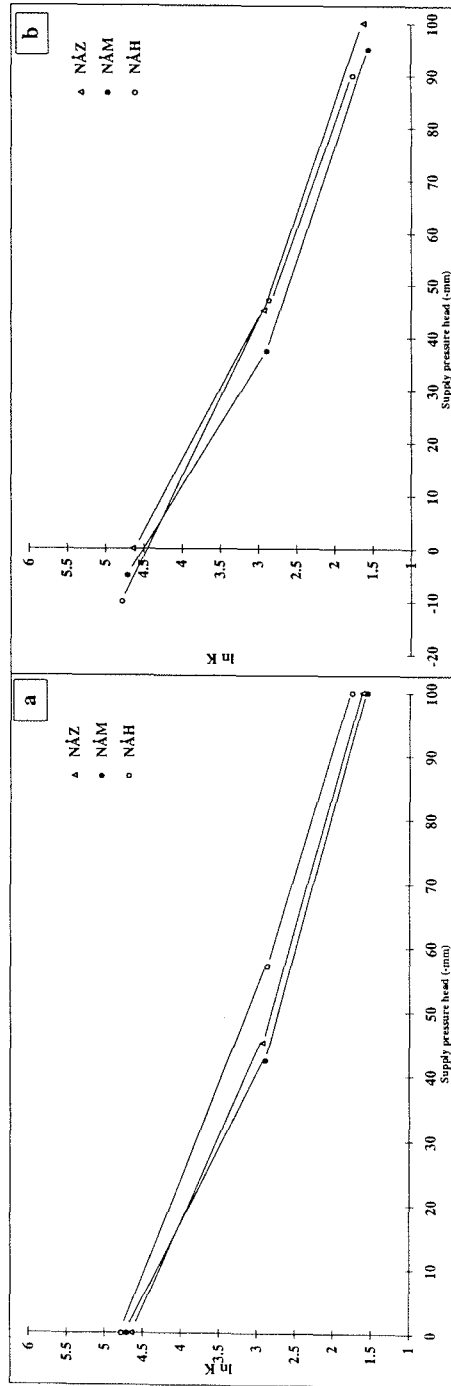


Figure 15. Comparison of regression lines in Figure 14 without adjustment (a) and with adjustment.

The geometry of the wetting fronts observed in the boxes NÅZ3, NÅM3 and NÅH3, after the last infiltration run at -1 cm water pressure head, is included in Table 5.

Table 5. Geometry of the wetting fronts in the boxes Nântuna soil (-1 cm water pressure head)

Slope	(%) :	0.0	12.5	25.0
Surface wetted diameter (cm):		28.0	31.0	37.0
Wetting depth	(cm):	12.0	9.5	5.5

A lateral expansion of the water bulb in the case of increasing slope gradient was thus observed.

5.3 Discussion

In section 3.2 some limitations of tension infiltrometers in their characterization of physical properties of surface soil were mentioned. Soil uniformity and homogeneity were assumed in the uppermost horizons (see Appendix 2: Soil description), in which infiltration takes place. In practice very few soils meet the homogeneity and isotropy requirements. Evidences of swelling and shrinkage processes did not exist in these alluvio-colluvial soils. Steady state flow was reached within reasonable time, moreover since each infiltration sequence was run at the same position within the plots.

Clearly, this study has not met the requirements of measurements with level device. Increasing slope gradient imposed some problems with the device stability to maintain full capillary contact with the soil surface. This problem was however overcome with stabilizing supports. In principle, tension infiltrometer tests should be run on a level surface, otherwise the supply pressure head will vary from the upslope to the downslope side (White *et al.*, 1992). A predetermined slightly negative supply pressure head (i.e. near saturation) for level measurements, may on sloping land impose positive supply pressure heads at the lower portion of the disc/soil interface. In the present studies, however, superficial water flow was never occurring.

On steep slope it may sometimes be necessary to create a “bench” (Sullivan *et al.*, 1996). However, this action implicates disturbance and removal of surface soil material, which may be of vital interest in studies of the impact of crust or sealing on infiltration rate.

Errors in actual supply pressure heads when measurements are carried out on sloping land may arise from the inclined free water surface in the bubble tower, and from the disc/soil interface (Appendix 4: *Slope adjustment of tension infiltrometer*). Figure 16 represents a comparison between adjusted and non-adjusted tests on the Nântuna soil taking account these deviation in supply pressure head.

At a slope of 25% (NÅH1, NÅH2 and NÅH3), the initial supply pressure heads used: -100, -60, -40, -20 and -10 mm, would be transformed to -97, -58.2, -38.8, -19.4 and -9.7 mm when adjusting for the inclined water face in the bubble tower. It is possible to observe (figures 16a and 16b) that the difference in the paired (ψ_b , K_b) boundary point is only [-2.167, +0.022], and in the $\ln K_{fs}$ only 0.0093. Therefore, with this adjustment, there was a negligible effect of inclination on the variation of the actual supply pressure head.

However, given the gravitational head difference that exist between upslope and downslope part at the disc/soil interface at the slope gradient 25%, the effects are larger (figures 16a and 16c). The predetermined supply pressure head is valid for the midpoint of the disc. In the lowest portion of the disc/soil interface, the supply total head will be approximately 24 mm higher and at the highest portion 24 mm lower, than in the middle.

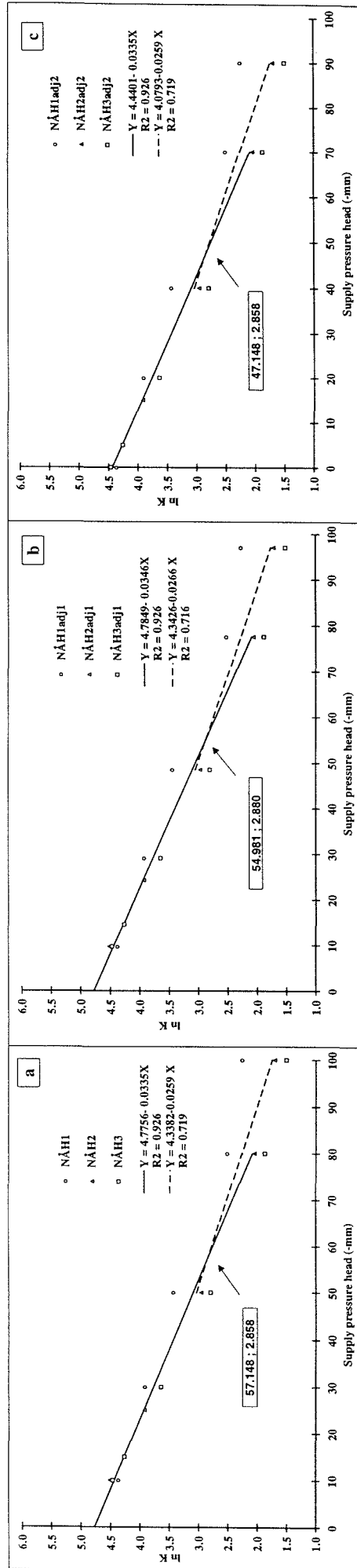


Figure 16. Comparison between non-adjusted (a), bubble tower adjustment (b) and disc/soil interface adjustment (c). Nantuna soil at 25% of slope.

Due to the exponential relationship of K (equation 4), the higher supply pressure heads at the lower part of the disc/soil interface will dominate the infiltration performance. If average total head is assumed midway between disc center and lower border, supply total heads will be approximately 10 mm higher than the predetermined for 25% slope and 5 mm higher for 12.5% slope. The 12.5% line will then move away from the zero line, whereas the 25% line will almost coincide with the zero line (Figure 15b). If average total head is assumed 2,5 cm higher than the predetermined below the disc center, i.e. supply total heads 5 mm (25% slope) and 2.5 mm (12.5% slope), all lines would coincide more with almost identical K_{fs} .

Applying the disc/soil interface adjustment for field work results, it is possible to observe (figures 17 and 18) changes in the $\ln K_{fs}$ and for the boundary point values. The maximum corrections made for average slope gradients (Table 6), will make the lines to move closer to each other, but not totally (see figures 11 and 19). The tendency in the $\ln K_{fs}$ to decrease with a reduction in the slope gradient, is similar to non-adjusted approach (Table 6). Thus, other factors than the slope gradient contribute to explain the differences in the field study (see also results of stepwise procedure in section 5.1).

Table 6. Changes in K_{fs} according to slope adjustment. North and south exposure soils

Plot	Initial $\ln K_{fs}$	Adjusted $\ln K_{fs}$	Initial K_{fs} (mm h^{-1})	Adjusted K_{fs} (mm h^{-1})	Average slope (%)	Slope range (%)
NL	2.70	2.30	14.88	9.95	13.3	10.5 - 15.7
NM	3.86	3.11	47.70	22.47	20.5	20.0 - 20.9
NH	4.02	3.24	55.84	25.54	27.7	26.4 - 28.7
SL	3.06	2.75	21.41	15.68	12.1	11.4 - 13.1
SM	4.19	3.76	66.02	43.06	15.4	14.2 - 17.4
SH	5.07	4.23	159.30	68.72	24.9	20.4 - 27.6

According to the classes recommended to indicate hydraulic conductivity (FAO, 1990), the north-facing soils presented moderately slow to moderately rapid K_{fs} values and the south-facing soils moderately rapid to rapid K_{fs} values (Table 6). In relation to the spatial variability observed, Warrick & Nielsen (1980) showed that the hydraulic conductivity requires a large sample number to be estimated with security. Moreover, the variation of actual slope gradient range, within each slope class (L, M, H) may in part explain the dispersion observed.

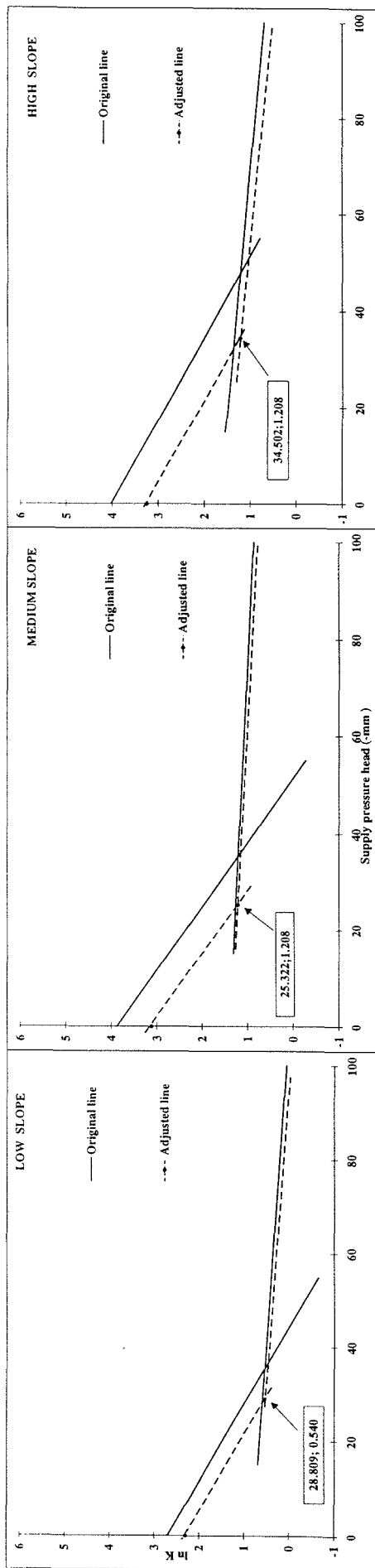


Figure 17. The adjusted straight line of the logarithm of hydraulic conductivity (mm h^{-1}). North-facing soils.

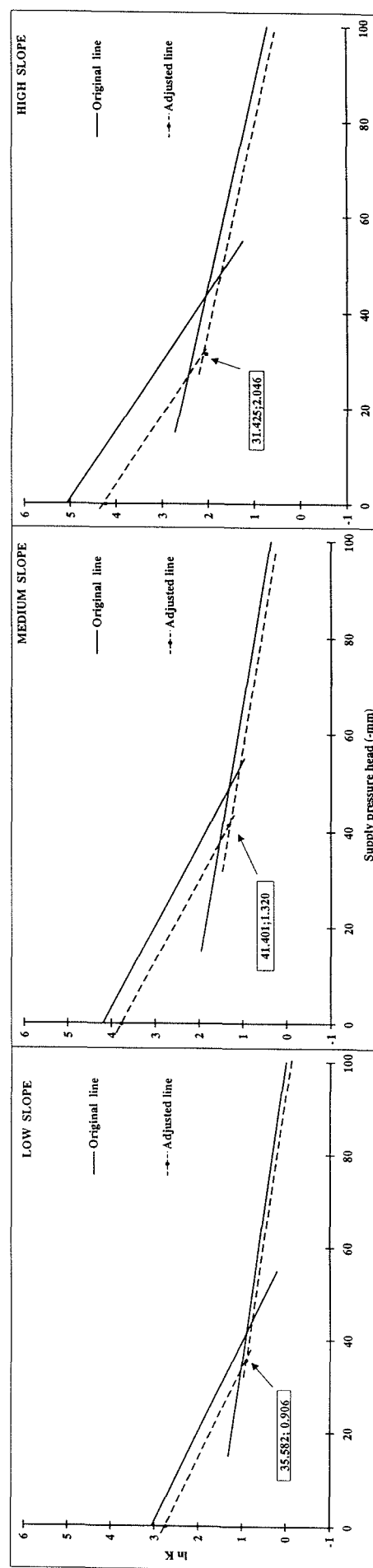


Figure 18. The adjusted straight line of the logarithm of hydraulic conductivity (mm h^{-1}). South-facing soils.

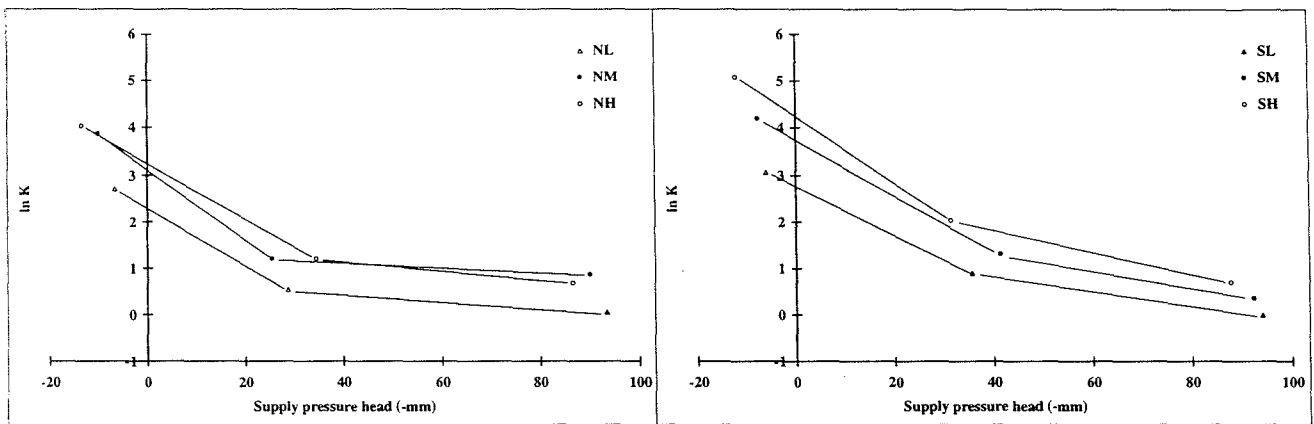


Figure 19. Disc/soil interface adjustment for field work measurements.

6. CONCLUSIONS

- In the rainfed area under study, the morphologic soil differences between hillsides (north and south exposure) led to differences in the soil infiltration parameters.
- The north-facing soils present moderately slow to moderately rapid field saturated hydraulic conductivity (K_{fs}) values and in the south-facing soils moderately rapid to rapid K_{fs} values.
- The spatial variability in the hydraulic conductivity estimates were high in field and laboratory studies.
- The unsaturated hydraulic conductivity [$K(\psi)$] had a tendency to increase when the slope gradient was increased. This tendency was observed both in the field (north and south exposure) and in laboratory.
- There were no significant effects of inclination on the variation of the supply pressure head, when considering the slope adjustment in the bubble tower.
- The gravitational head difference produced between upslope and downslope device sides was proportional to the slope magnitude. However, the tendency in $K(\psi)$ observed in the field was maintained.
- The results were attributed to the differences in the vertical and lateral hydraulic conductivity in the field soils, and to the occurrence of surface sealing in the plots at low slope gradients.
- According to multiple stepwise regression analysis, the $K(\psi)$ parameters were fundamentally determined by the slope gradient of the hillside and the proportion of texture separates in the surface soil.

7. REFERENCES

- Agassi, M., Shainberg, I. and Van der Merwe, D. 1994. Effect of water quality on inter-rill erosion and infiltration : laboratory study. *Australian Journal of Soil Research* 32: 595 -601.
- Ankeny, M. D., Ahmed, M., Kaspar, T. C. and Horton, R. 1991. Simple field method for determining unsaturated hydraulic conductivity. *Soil Science Society of American Journal* 55: 467 - 470.
- Beven, K. and German, P. 1982. Macropores and water flow in soils. *Water Resource Research* 18: 1311 - 1325.
- Black, C.A. 1965. *Methods of soil analysis*. American Society of Agronomy. Agronomy Monograph no. 9. Madison, WI. USA. Vol. 2. 1572 p.
- Blake G. R. and Hartge, K. H. 1986a. Bulk density. pp: 363 - 382. In: *Methods of soil analysis. Part 1. Physical and Mineralogical Methods*. 2nd ed. (Klute, A. Ed.). Agronomy Monograph no. 9. Madison, WI. 1188 p.
- Blake G. R. and Hartge, K. H. 1986b. Particle density. pp: 377 - 382. In: *Methods of soil analysis. Part 1. Physical and Mineralogical Methods*. 2nd ed. (Klute, A. Ed.). Agronomy Monograph no. 9. Madison, WI. 1188 p.
- Börgel, R. 1966. Geomorfología cuaternaria de la cuenca de Santiago. pp: 41-54. In: *Estudios geomorfológicos. Homenaje Facultad de Filosofía y Educación a Don Humberto Fuenzalida*. 184 p
- Bronstert, A. and Plate, E. J. 1997. Modelling of runoff generation and soil moisture dynamics for hillslopes and micro-catchments. *Journal of Hydrology* 198: 177 - 195.
- Brügen, J. 1950. *Fundamentos de la Geología de Chile*. Instituto Geográfico Militar de Chile. 374 p.
- Cerdà, A. 1996. Seasonal variability of infiltration rates under contrasting slope conditions in southeast Spain. *Geoderma* 69: 217 - 232.
- Cerdà, A. 1997. Seasonal changes of infiltration rates in a Mediterranean scrubland on limestones. *Journal of Hydrology* 198: 209 - 225.
- Chile-Comisión Nacional de Riego. 1981. *Estudio Agrológico del Proyecto Maipo (Scale 1:20.000)*. Agrológ Ltda. 4 v. (texts and maps).
- Chile-Comisión Nacional de Riego. 1987. *Estudio Agroclimático del Proyecto Maipo*. Corporación Privada para el Desarrollo de las Ciencias Agropecuarias. Santiago. Chile. 221 p.
- Cook, F. J., Lilley, G. P. and Nunns, R. A. 1993. Unsaturated Hydraulic Conductivity and Sorptivity: Laboratory Measurements. pp: 615- 624. In: Carter, M. R. (Ed.) *Soil Sampling and Methods of Analysis*. Canadian Society of Soil Science. Lewes Publishers. 823 p.

- Cook, F. J. and Broeren A. 1994. Six methods for determining sorptivity and hydraulic conductivity with disc permeameter. *Soil Sciences* 157: 2 - 11.
- CSIRO, 1988. CSIRO disc permeameter. Instruction Manual. Centre for Environmental Mechanics. Canberra. 31 p.
- Dirksen, C. 1991. Unsaturated Hydraulic Conductivity. pp: 209- 269. *In: Smith, K. A. and Mullins, C. E. (Eds.). Soil analysis: physical methods.* Marcel Dekker Inc. New York. 620 p.
- FAO, 1990. Guidelines for soil description. 3rd Edition (Revised). Food and Agriculture Organization of the United Nations. Rome. 70 p.
- Gang Li, Shiu Hung Luk and Qiang Guo Cai. 1995. Topographic zonation of infiltration in the hilly loess region, North China. *Hydrological Process* 9 : 227 - 235.
- Gardner, W. R. 1958. Some steady state solutions of the unsaturated flow equation with application to evaporation from a water table. *Soil Science* 85: 228 - 232.
- Gee G. W. and Bauder, J. W. 1986. Particle-size analysis. pp: 383 - 411. *In: Methods of soil analysis. Part 1. Physical and Mineralogical Methods.* 2nd ed. (Klute, A. Ed.). Agronomy Monograph no. 9. Madison, WI. 1188 p.
- Hanna, Y. A., Harlan, P. W. and Lewis, D. T. 1982. Soil available water as influenced by landscape position and aspect. *Agronomy Journal* 74: 999 - 1.004.
- Hillel, D. 1982. Introduction to Soil Physics. Department of Plant and Soil Sciences, University of Massachusetts, Amherst. Academic Press, Inc. 364 p.
- Jackson, C. R. 1992. Hillslope infiltration and lateral downslope unsaturated flow. *Water Resource Research* 28: 2.533 - 2.539.
- Kim, K.H. and Miller, W.P. 1996. Effect of rainfall electrolyte concentration and slope on infiltration and erosion. *Soil Technology* 9: 173 - 185.
- Keng, J. C. W. and Lin, C. S. 1982. A two-line approximation of hydraulic conductivity for structured soils. *Canadian Agricultural Engineering* 24 (2): 77 - 80.
- Linnér, H. 1984. The influence of soil moisture on evapotranspiration, growth, nutrient uptake, yield and quality of the potato (*Solanum tuberosum* L.). Swedish University of Agricultural Sciences. Department of Soil Science. Division of Hydrotechnics. Rapport and Dissertation 142. 153 p.
- Longsdon, S. E. and Jaynes, D.B. 1993. Methodology for determining hydraulic conductivity with tension infiltrometer. *Soil Science Society of American Journal* 57: 1.426 - 1.431.
- Luk, S. H., Cai, Q. G. and Wang, G. P. 1993. Effects of surface crusting and slope gradient on soil and water losses un the hilly loess region, north China. *Catena Supplement* 24: 29 - 45.
- Mahler, R. L., Bezdicek, D. F. and Witter, R. E. 1979. Influence of slope position on nitrogen fixation and yield of dry peas. *Agronomy Journal* 71: 348 - 351.

- Manning, R. 1891. On the flow of water in open channels and pipes. Trans. Inst. Civil Eng. Ireland 20: 161 - 207.
- Marshall, T. J. and Holmes, J. W. 1992. Soil Physics. Reprinted 2nd ed. Cambridge University Press. Australia. 374 p.
- McLaren, R. C. and Cameron, K. C. 1996. Soil Science. Sustainable production and environment protection. 2nd Edition. Oxford University Press, New Zealand. 304 p.
- Messing, I. 1993. Saturated and Near-Saturated Hydraulic Conductivity in Clay Soils. Measurement and Prediction in Field and Laboratory. PhD Thesis. Swedish University of Agriculture Sciences, Department of Soil Sciences. Uppsala, Report and Dissertation N° 12. 66 p.
- Messing, I. and Jarvis, N. J. 1993. Temporal variation in the hydraulic conductivity of a tilled clay soil as measured by tension infiltrometer. Journal of Soil Science 44: 11 - 24.
- Mwendera, E. J. and Feyen, J. 1993. Tillage and rainfall effects on infiltration and predictive applicability of infiltration equations. Soil Science 156 : 20 - 27.
- Philip, J.R. 1957. The theory of infiltration. IV. Sorptivity and algebraic infiltration equations. Soil Science 84: 257 - 264.
- Philip, J.R. 1969. Theory of infiltration. Advances in Hydrosience 5: 215 - 296.
- Philip, J.R. 1991. Constant rainfall infiltration into bounded shallow profiles. Water Resource Research 27: 3265 - 3270.
- Reynolds, E. D. and Elrick, D. E. 1991. Determination of hydraulic conductivity using tension infiltrometer. Soil Science Society of America Journal 55: 633 - 639.
- Reynolds, W. D. 1993. Unsaturated Hydraulic Conductivity: Field Measurements. pp: 633-644. In: Carter, M.R. (Ed.) Soil Sampling and Methods of Analysis. Canadian Society of Soil Science. Lewis Publishers. 823 p.
- Ritsema, C. J., Oostindie, K. and Stolte, J. 1996. Evaluation of vertical and lateral flow through agricultural loessial hillslopes using a two-dimensional computer simulation model. Hydrological Processes 10: 1.091 - 1.105.
- Shainberg, I., Rhoades, J. D. and Prather, R. J. 1981. Effect of low electrolyte concentration on clay dispersion and hydraulic conductivity of a sodic soil. Soil Science Society of American Journal 45: 273- 277.
- Smith, R. E. 1972. The infiltration envelope: results of a theoretical infiltrometer. Journal of Hydrology 17: 1 -21.
- Sullivan, M., Warwick, J. J. and Tyler, S. W. 1996. Quantifying and delineating spatial variations of surface infiltration in a small watershed. Journal of Hydrology 181: 149 -168.
- Thomas, G. W. and Phillips, R. E. 1979. Consequences of water movement in macropores. Journal of Environmental Quality 8: 149 - 152.

Warrick, A. W., Wierenga, P. J. and Pan, L. 1997. Downward water flow through sloping layers in the vadose zone: analytical solutions for diversions. *Journal of Hydrology* 192: 321 - 327.

Warrick, A. W. and Nielsen, D. R. 1980. Spatial variability of soil physical properties in the field. pp: 319 - 344. In : *Applications of Soil Physics*. Hillel, D. (Ed.). Academic Press Inc. 385 p.

White, I. and Perroux, K. M. 1987. Use of sorptivity to determine field soil hydraulic properties. *Soil Science Society of American Journal* 51: 1093 - 1101.

White, I., Sully, M. J. and Perroux, K. M. 1992. Measurement of Surface-Soil Hydraulic Properties: Disk Permeameter, Tension Infiltrometer, and Other Techniques. pp: 69- 103. In : G. C. Topp *et al.* (Ed.). *Advances in Measurements of Soil Physical Properties: Bringing Theory into Practice*. S. S. S.A., Special Publication N° 30. S.S.S.A., Madison, WI. USA. 288 p.

Wooding, R. A. 1968. Steady infiltration from a circular pond. *Water Resource Research* 4: 1259 - 1273.

APPENDIX 1

CLIMATE

According to Maipo's Project, an Agro-climatic Survey (Chile-Comisión Nacional de Riego, 1987), the Germán Greve Silva Experimental Station is included in the agro-climatic district *Santiago* (IV.1). Its physiographic position is the Central Valley and its main localities are Quillota, *Maipú*, Santiago, Calera de Tango, Buin, Paine:

i	17	29	c	13	3
h	11	0.01	c	1	1.88

where:

Thermic characteristics (upper part) :

- i = 9 months freeze-free.
- 17 = between 1700 and 2000 annual degree days.
- 29 = between 29.0 and 29.9°C, January maxim temperature.
- c = 3 month of vegetative recess.
- 13 = between 1300 and 1399 annual freezing hours.
- 3 = between 3.0 and 3.9°C, July minimum temperature.

Hydric characteristics (lower part) :

- h = 8 dry months.
- 11 = between 1100 and 1199 mm annual water deficit.
- 0.01 = summer moisture index (PP/ETP=0.01).
- c = 3 moist months.
- 1 = between 100 and 199 mm annual water excess.
- 1.88 = winter moisture index (PP/ETP=1.88).

Table 7. Thermic characteristics in Santiago District, Chile (33° SL -71° W.L.)

	J	F	M	A	M	J	J	A	S	O	N	D	YEAR
Tmax (°C)	29.3	28.3	25.5	21.7	17.9	15.1	14.1	15.1	17.9	21.7	25.5	28.3	21.7
Tmin (°C)	11.7	11.2	9.6	7.6	5.5	4.0	3.5	4.0	5.6	7.6	9.7	11.2	7.6
Tmean (°C)	19.6	18.8	16.8	14.0	11.2	9.2	8.4	9.2	11.2	14.0	16.8	18.8	14.0

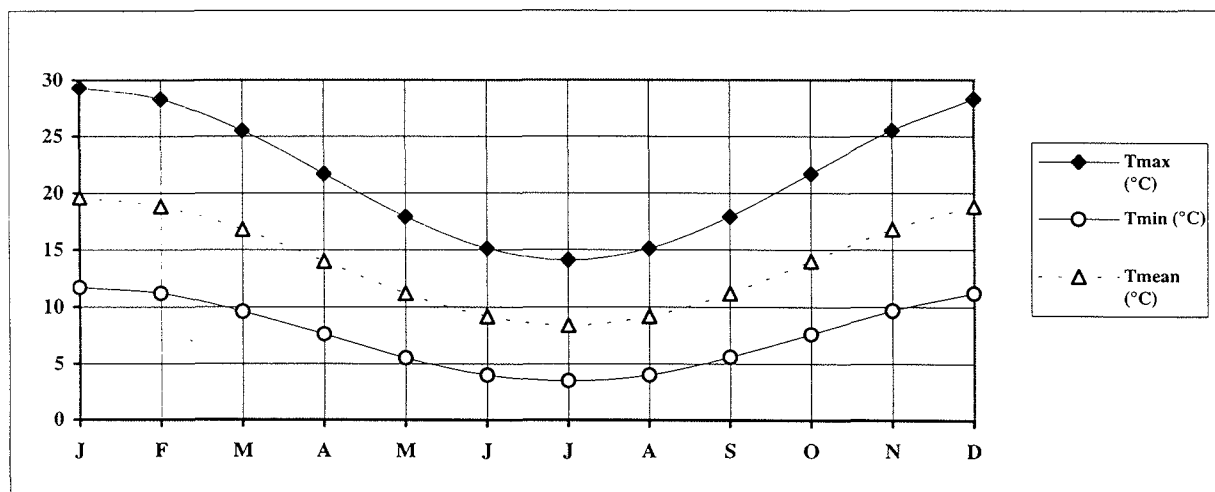


Table 8. Hydric characteristics in Santiago District, Chile (33° SL -71° W.L.)

	J	F	M	A	M	J	J	A	S	O	N	D	YEAR
Pp mean(mm)	2.6	3.0	4.0	16.3	63.9	82.3	69.2	60.0	22.3	12.8	5.8	2.8	345
Pp 1996(mm)			0.0	36.3	6.8	37.5	26.3	26.3	0.0				133.2
RH (%)	59	61	65	71	76	80	82	80	76	70	65	61	71
ETP (mm)	197.0	185.8	155.2	113.5	71.7	41.2	30.0	41.2	71.8	113.5	155.3	185.8	1362

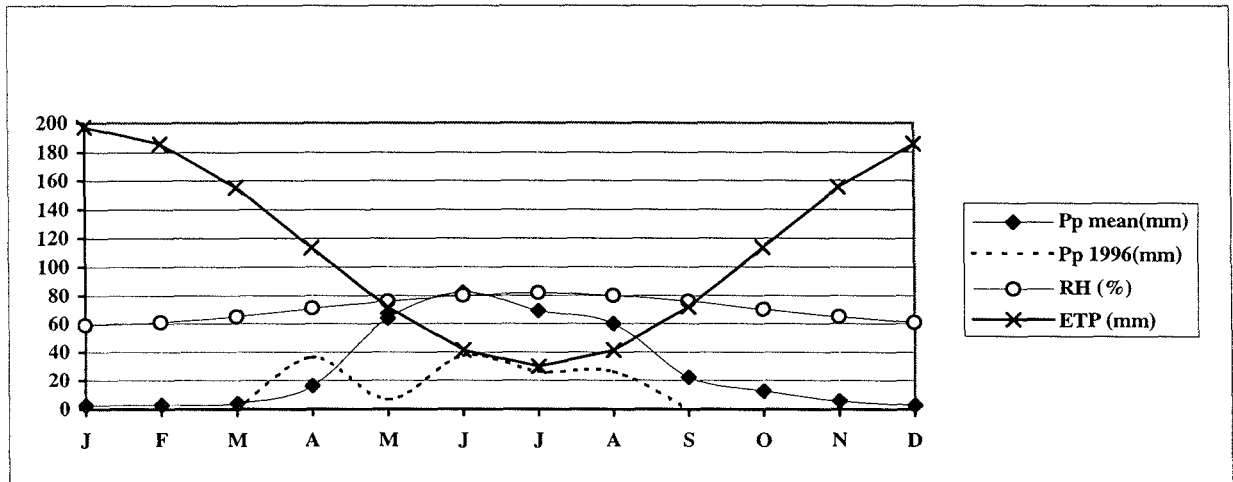
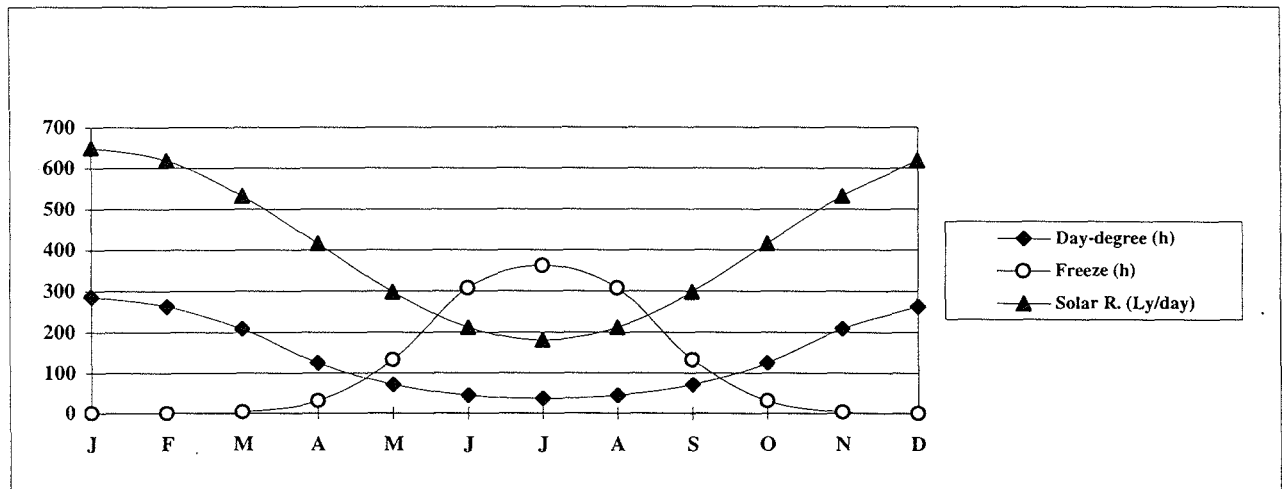


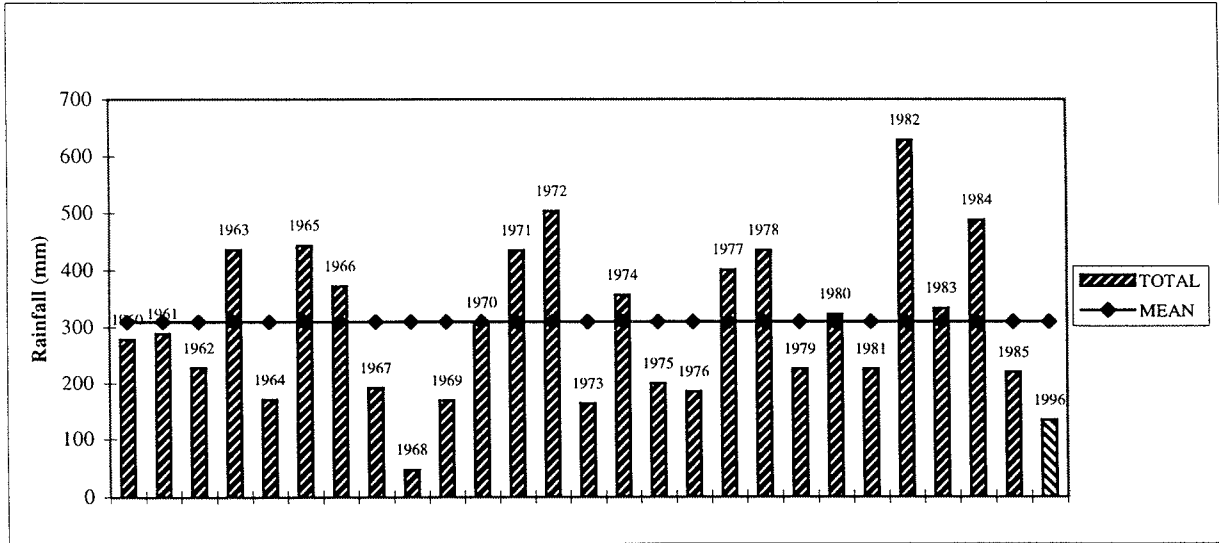
Table 9. Other agro-climatic features in Santiago District, Chile (33° SL -71° W.L.)

	J	F	M	A	M	J	J	A	S	O	N	D	YEAR
Day-degree (h)	286	263	209	124	71	44	36	44	71	124	209	263	21.7
Freeze (h)	0	0	3	31	132	307	361	307	132	31	3	0	7.6
Solar R. (Ly/day)	649	618	532	415	298	212	181	212	298	415	532	618	415

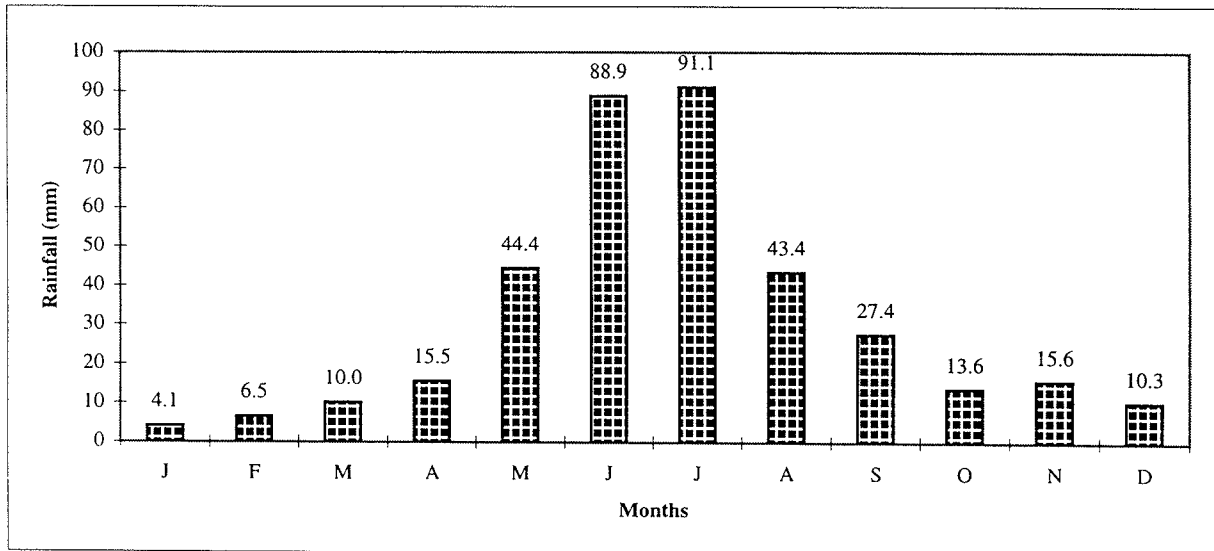


Study area rainfall.

The next figure shows annual rainfall for a 25 years period, between 1960 and 1985, in the Germán Greve E.S. The rainfall during this period can be compared with the the mean precipitation, which is 309.5 mm.



On other hand, the next figure describes the monthly average of precipitation for the same period in the Germán Greve E. S.



APPENDIX 2



WATERSHED TOPOGRAPHIC SURVEY		
"GERMAN GREVE" AGRICULTURAL EXPERIMENT STATION (CHILE)		
AGRICULTURAL AND FORESTRY FACULTY - UNIVERSIDAD DE CHILE		
PROJECT NAME : AGROFORESTRY UNDER RUNOFF FARMING TO ENHANCE		
SUSTAINABLE AGRICULTURE PRODUCTION OF FOOD AND FIREWOOD IN DRYLAND		
JANUARY / 1996	Surveyors : CASTRO, M., MALDONADO, P. and VERGARA, J.	SURFACE 74.6 ha
SCALE	Calculated and revised : CASANOVA, M	33°28' L.S. 70°50' L.W

APPENDIX 3

SOIL DESCRIPTION

1. GENERAL INFORMATION

1.1 Registration and location.

- 1.1.1 *Profile number:* AMCHS1 = south exposure
AMCHN1 = north exposure
- 1.1.2 *Soil profile description status :* Reference profile description
- 1.1.3 *Date of description :* 970115
- 1.1.4 *Author :* Manuel Casanova
- 1.1.5 *Soil unit :* Soil Serie *Piedmont Cuesta de Barriga*
- 1.1.6 *Location :* Southamerica, Chile, Santiago, Province of Santiago, Comune of Maipú. North and south exposure hillside of a microbasin in the Experimental Station Germán Greve Silva; in the area of Ovine Research Program belonging to Husbandry Department of the Agricultural and Forestry Faculty of Universidad de Chile. Local name is "Rincón Pajaritos".
- 1.1.7 *Elevation :* 500 (asl)
- 1.1.8 *Map sheet number and grid reference*
Pudahuel 332230 - 704500
Scale = 1: 25.000
Sheet E-57 Pudahuel S.E.
UTM:
Abcise origin (E) meridian 69 West =
500 km
Ordinate origin (N) 10.000 km at south
of Equator
Key location in the chart 1: 1.000.000 SI-19-1-
c-3-14.
Altimetric readings : average sea level.
- 1.1.9 *Coordinates:* 33° 28' SL - 70° 50' WL.

1.2 Soil Classification :

1.2.1 *Soil Taxonomic Classification*

Soil Taxonomy : Coarse loamy, mixed, thermic Typic Xerochrepts

1.2.2 *Soil climate:*

Soil temperature regime = thermic
Soil moisture regime = xeric
Annual Precipitation = 330 mm
Average annual temperature = 14.2°C

1.3 Landform and Topography

- 1.3.1 *Topography :* Hilly (slope 15 - 30%) to steeply dissected (> 30%).
- 1.3.2 *Landform :* Microbasin
- 1.3.3 *Land element:* North and south slope

1.3.4 **Position :** Lower and middle slope

1.3.5 **Slope :**

Gradient = moderately steep to steep (15- 30% to 30-60%)
Form = concave.

1.3.6 **Micro-topography:** Animal burrows (caviomorph rodent, Octodontidae family, *Octodon degus*)

1.4 Land Use and Vegetation

1.4.1 **Land use :** Animal husbandry, extensive grazing.

1.4.2 **Human influence :** Burning and clearing.

1.4.3 **Vegetation :** Savanna (grasses with a discontinuous layer of *Acacia cavens* trees or xeromorphic shrubs) with an grass cover between 15 and 40%.

1.5 Parent Material

1.5.1 **Parental material :** Granitic and granidioritic colluvial deposits with alluvial influence

1.5.2 **Effective soil depth :** Moderately deep (60 -75 cm)

1.6 Surface Characteristics

1.6.1 **Rocks Outcrops :** None.

1.6.2 **Surface coarse fragment :** Angular and subangular fine to coarse gravel, common (5 - 10%) in south exposure and many (20 - 30 %) in north exposure.

1.6.3 **Erosion :**

	North exposure	South exposure
Main categories :	1° Water erosion 2° Wind and mass movement	1° Mass movement 2° Water and wind erosion
Types :	Sheet	Landslides
Degree :	Moderate	Slight
Activity :	Active in recent past (< 100 years)	Active at present

1.7 Soil-Water Relationships

1.7.1 **Drainage classes :** Well drained.

1.7.2 **Internal drainage :** Moderately slow.

1.7.3 **External drainage :** Rapid run-off.

1.7.4 **Flooding :** None flooding.

1.7.5 **Groundwater :** Not observed

1.7.6 **Moisture condition :** Dry in all the profile.

SOIL PROFILE DESCRIPTIONS

North exposure profile

0 - 15 cm

A

Brown to dark brown (10 YR 4/3)_a, very dark greyish brown (10 YR 3/2)_m; silty clay loam; moderate medium and fine subangular blocks, breaking to strong fine and medium granular structure; very plastic, very sticky and hard; common fine and very fine roots; few fine and very fine interstitial pores; abundant subrounded fine gravel, common coarse angular gravel. Smooth and diffuse boundary.

15 - 62 cm

Bw

Dark greyish brown (10 YR 4/2)_a, very dark grey to very dark greyish brown (10 YR 3/1 to 10 YR 3/2)_m; silty clay; strong fine and medium subangular blocks; very plastic, very sticky and hard; common medium and fine roots; abundant coarse, medium, fine and very fine interstitial pores; angular coarse gravel (2- 3 cm; 15 %). Smooth and diffuse boundary.

62 - 93 cm

BC

Slight brown to reddish yellow (7.5 YR 6/5)_a, brown to dark brown (7.5 YR 4/4)_m; silty clay loam; weak medium and fine angular blocks, trending to massive; plastic, very sticky and extremely hard; no roots; few fine and very fine interstitial pores; abundant angular fine and coarse gravel, abundant subrounded stones. Smooth and diffuse boundary

93 - 114 cm

C

Slight yellowish brown (10 YR 6/4)_a, yellowish brown (10 YR 5/6)_m; sandy clay loam; massive; plastic, very sticky and extremely hard; no roots; common fine and very fine interstitial pores; abundant fine gravel, many coarse gravel. Smooth and gradual boundary.

114- 158 cm

IIC

Slight yellowish brown (10 YR 6/4)_a, dark yellowish brown (10 YR 4/4)_m; silty clay loam; massive; plastic, very sticky and extremely hard; no roots; very few interstitial pores; common coarse, medium and fine gravel.

South exposure profile

0 - 24 cm

A

Brown to dark brown (10 YR 4/4)_a, dark brown (10 YR 3/3)_m; silty clay; moderate medium and fine subangular blocks, breaking to strong fine and granular structure; very plastic, very sticky and hard; common fine and very fine roots; common medium, abundant fine and very fine, few coarse interstitial pores; many coarse gravel. Wavy and abrupt boundary.

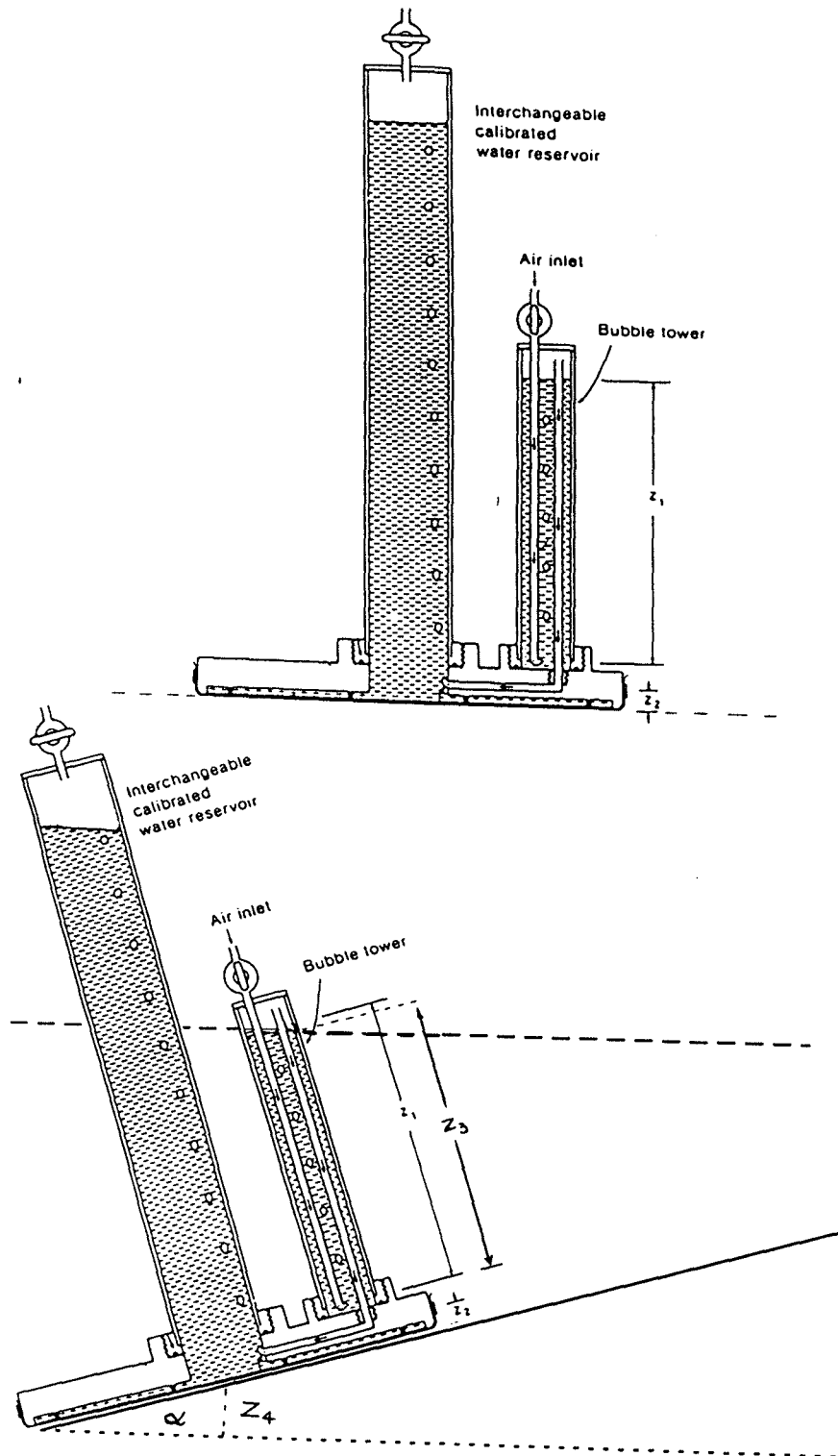
24 - 70 cm

Bt

60% yellowish red (5YR 4/6)_a, 40% dark reddish brown (5 YR 3/3)_a; 60% reddish brown to yellowish red (5 YR 4/5)_m, 60% dark reddish brown (5 YR 3/2); clay; strong coarse and medium prismatic structure; very plastic, very sticky and extremely hard; abundant fine and very fine roots; abundant fine and very fine interstitial pores; many medium (< 2 cm) vertical cracks along the horizon; few and very few fine and medium angular gravel (<5 %).

APPENDIX 4

SLOPE ADJUSTMENT OF TENSION INFILTRMETER



Förteckning över utgivna häften i publikationsserien

SVERIGES LANTBRUKSUNIVERSITET, UPPSALA. INSTITUTIONEN FÖR MARKVETENSKAP.
AVDELNINGEN FÖR LANTBRUKETS HYDROTEKNIK. AVDELNINGSMEDDELANDE. Fr o m 1995

- 95:1 Alavi, G. Radial stem growth and transpiration of Norway spruce in relation to soil water availability. Granens tillväxt och transpiration i relation till markvattnets tillgänglighet (Licentiatavhandling). 13 + 11 + 14 s.
- 95:2 Johansson, W. & Fellin, O. Biogas från vall. Teknik och ekonomi vid odling, skörd, transporter, ensilering samt rötning med tvåstegsteknik. 38 s.
- 95:3 Svensson, E., Linnér, H. & Carlsson, H. Utvärdering av växtanalys i fabrikspotatis. 53 s.
- 95:4 Andersson, A. Vattentillgångar för bevattning i Kalmar län. I. Litteraturoversikt. II. Intervjuundersökning rörande vattenmagasin. 48 s.
- 95:5 Wesström, I. Bestämning av markens salthalt genom mätning med konduktivitetssond. 18 s.
- 95:6 Eckersten, H., Jansson, P-E., Karlsson, S., Persson, B., Perttu, K. & Andersson, J. En introduktion till biogeofysik. 72 s.
- 95:7 Eckersten, H. Simulation of water flow in plant communities. SPAC model description, exercises and user's manual. 49 s.
- 95:8 Nabieian, F. Simulering av vattenbalans för energiskog på en torvmark. 25 s.
- 96:1 Eckersten, H., Jansson, P-E., & Johnsson, H. SOILN model, user's manual. Version 9.1. 93 s.
- 96:2 Eckersten, H., Jansson, P-E., Karlsson, S., Lindroth, A., Persson, B., Perttu, K. & Andersson, J. En introduktion till biogeofysik, 2:a upplagan. 110 s.
- 96:3 Carlsson, H., Larsson, K. & Linnér, H. Växtnäringsstyrning i potatis. 69 s.
- 97:1 Uppenberg, S., Wallgren, O. & Åhman, M. Saturated hydraulic conductivity in an acid sulphate soil. A minor field study in the the Vietnamese Mekong delta. 45 s.
- 97:2 Djodjic, F. Avrinningsmönster i ett litet åkerområde under 40 år av successiv urbanisering. 38 s.
- 97:3 Vukovic, M. The effect of soil hydraulic properties on ground water fluctuations in a heavy clay soil. Measurements and simulations. 43 s.
- 97:4 Eckersten, H., Jansson, P-E., Karlsson, S., Lindroth, A., Persson, B., Perttu, K., Carlsson, M., Lewan, L. & Blombäck, K. En introduktion till biogeofysik, 3:e upplagan. 130 s.
- 97:5 Eckersten, H. Simulation of water flow in plant communities. SPAC model description, exercises and user's manual. 2nd edition. SPAC version 5.0. 52 s.
- 98:1 Lustig, T. Land Evaluation Methodology. Small-Scale Agro-Pastoralist Farming Systems. Agricultural community case study in the IV region of Chile. 91 s.
- 98:2 Jansson, P-E. Simulating model for soil water and heat conditions. Description of the SOIL model. 81 s.
- 98:3 Casanova, M. Influence of slope gradient and aspect on soil hydraulic conductivity measured with tension infiltrometer. Field study in the Central Zone of Chile. 50 s.

Denna serie meddelanden utges av Avdelningen för lantbrukets hydroteknik, Sveriges Lantbruksuniversitet, Uppsala. Serien innehåller sådana forsknings- och försöksredogörelser samt andra uppsatser som bedöms vara av i första hand internt intresse. Uppsatser lämpade för en mer allmän spridning publiceras bl a i avdelningens rapportserie. Tidigare nummer i meddelandeserien kan i mån av tillgång levereras från avdelningen.

This series of Communications is produced by the Division of Agricultural Hydrotechnics, Swedish University of Agricultural Sciences, Uppsala. The series consists of reports on research and field trials and of other articles considered to be of interest mainly within the department. Articles of more general interest are published in, for example, the department's Report series. Earlier issues in the Communications series can be obtained from the Division of Agricultural Hydrotechnics (subject to availability).

Distribution:

Sveriges Lantbruksuniversitet
Institutionen för markvetenskap
Avdelningen för lantbrukets hydroteknik
Box 7014
750 07 UPPSALA

Swedish University of Agricultural Sciences
Department of Soil Sciences
Division of Agricultural Hydrotechnics
P.O. Box 7014
S-750 07 UPPSALA, SWEDEN

Tel. 018-67 11 85, 67 11 86

Tel. +46-(18) 67 11 85, +46-(18) 67 11 86
